

## Reassessment of the age and depositional environment of the Kırkgeçit Formation based on larger benthic foraminifera, NW Elazığ, Eastern Turkey

Sibel KAYGILI\* 

Department of Geological Engineering, Faculty of Engineering, Firat University, Elazığ, Turkey

Received: 01.02.2021

Accepted/Published Online: 30.07.2021

Final Version: 28.09.2021

**Abstract:** The middle-upper Eocene Kırkgeçit Formation, the fossil content of which is the subject of this study, is deposited in a back-arc basin controlled by block-faulting. The Kırkgeçit basin is interpreted as being formed under an extensional regime related to convergence between the Anatolian plate in the north and the Arabian plate in the south. The aim of this study is to reassess the age and depositional environment of the Kırkgeçit Formation by using detailed biometric analysis data obtained from the reticulate *Nummulites* and determinations of other larger benthic foraminifera (LBF) in the unit. For this purpose, two sections were measured from the latest Bartonian-Priabonian aged unit. Biometric data of the *Nummulites hormoensis* and *Nummulites fabianii* from the Kırkgeçit Formation exposures in the northwest of Elazığ has been presented for the first time. In general, *Nummulites fabianii* has robust test with thick walls, while *Nummulites hormoensis* has elongated test with thinner walls in relation to the increase of water depth. The change in embryon size of these reticulate *Nummulites* has been considered an important indicator for evolution and biostratigraphy. *Nummulites hormoensis* marks latest Bartonian to early Priabonian (SBZ 18) while *Nummulites fabianii* is a marker for middle-late Priabonian (SBZ 19-20).

The Kırkgeçit Formation in the study area was previously dated as late Lutetian-Priabonian based on LBF of it. However, by considering the LBF determined in this study, the latest Bartonian-Priabonian age was assigned to unit. Based on the paleontological and sedimentological features, the Kırkgeçit Formation has been interpreted as a unit deposited on the inner and middle parts of a shallow ramp.

**Key words:** Kırkgeçit Formation, latest Bartonian-Priabonian, eastern Turkey, reticulate *Nummulites*, biometry, paleoenvironment.

### 1. Introduction

The larger benthic foraminifera (LBF) discussed in this study are distinctive indicators of carbonates deposited in a shallow marine environment. For the Paleogene period, the content of benthic foraminifera in carbonate rocks, the subject of this study, is important in determining the depositional environment (Racey, 1995; Beavington-Penney and Racey, 2004; Jorry et al., 2006).

Around the Bartonian-Priabonian boundary corresponds to a major faunal turnover in the Tethyan shallow marine ecosystems (Cotton et al., 2017; Özcan et al., 2019b). Some new foraminiferal taxa, such as *Heterostegina*, *Pellatispira*, *Silvestriella* appear for the first time, while major groups of large *Nummulites* and alveolinids disappear during Bartonian and early Priabonian (Less and Özcan, 2012; Serra-Kiel et al., 2016; Özcan et al., 2018; Özcan et al., 2019a, b). Several groups, such as reticulate *Nummulites* and genus *Heterostegina*, *Spiroclypeus* in the peri-Mediterranean region appear to have the potential for a better biostratigraphic subdivision of shallow marine deposits in regard to their morphological changes recorded in the internal part of the test and their morphometric characterization (Less and Özcan, 2008; Less et al., 2008; Özcan et al., 2019a).

Reticulate *Nummulites* are common in the late middle and upper Eocene shallow marine deposits in Tethys. Because of characteristic features of the test surface, the identification of the group among the nummulids is rather easy, though the species concept is complicated (Papazzoni, 1998; Less and

Özcan, 2012; Cotton et al., 2015). Reticulate *Nummulites* (*Nummulites fabianii* lineage) occur from the late Lutetian to early Chattian in Tethys (Less et al., 2018). Reticulate *Nummulites*, whose evolution is poorly understood, are a distinctive and widespread group of *Nummulites*, commonly used in biostratigraphy (Cotton et al., 2015). The proloculus size of the megalospheric forms of reticulate species has been used in the determination of *Nummulites fabianii*-*Nummulites fichteli* lineage in the western Tethys. At the same time "The increase of the average length of chambers in the third whorl has secondary importance in recognizing the evolution of the reticulate *Nummulites* because it is affected also by ecological factors" (Özcan et al., 2019b, p.5).

The studies carried out in the Elazığ vicinity (Özkul, 1988; Özkul and Kerey, 1996; Cronin et al., 2000b; Aksoy et al., 2005) the age of the Kırkgeçit Formation is accepted as middle Eocene-Oligocene. In this study, the LBF content of the outcrops in the northwest of the Elazığ has been discussed.

Paleontological studies of Eocene LBF of the Kırkgeçit Formation in the northwest of Elazığ have been extremely limited (Avşar, 1983, 1991, 1996) (Table 1). The available data in relation to foraminiferal content of this unit is insufficient for a clear interpretation of biostratigraphic framework. The present information on the foraminiferal content of this unit is also either very poor or obsolete for a high-resolution biostratigraphic framework. For this reason, with this study, it is aimed to reassess the age and depositional environment of the Kırkgeçit Formation by using the data from detailed

\* Correspondence: skaygili@firat.edu.tr

**Table 1.** The correlation of benthic foraminifera assemblages and age assignments of the Kırkgeçit Formation in the previous studies and the present study.

Author	Benthic foraminifera assemblages	Age
Avşar, 1983	<i>Nummulites fabianii</i> , <i>N. perforatus</i> , <i>N. striatus</i> , <i>Assilina spira</i> , <i>Sphaerogypsina globula</i> , <i>Asterigerina rotula</i> , <i>Eorupertia magna</i> , <i>Halkyardia minima</i> , <i>Fabiania cassis</i> , <i>Chapmanina gassinensis</i> , <i>Linderina brugesii</i> , <i>Silvestriella tetraedra</i> , <i>Alveolina fusiformis</i> , <i>A. elongata</i> , <i>Praebullalveolina afyonica</i> , <i>Praerhapydionina huberi</i> , <i>Peneroplis damesini</i> , <i>P. dusenburyi</i> , <i>P. aff. laevigatus</i> , <i>Spirolina aff. cylindracea</i> , <i>Maslinella aff. chapmani</i> , <i>Peneroplis sp.</i> , <i>Austrotrillina sp.</i> , <i>Planorbulinidae</i> , <i>Rotaliidae</i> .	Upper Lutetian-Priabonian
Avşar, 1991	<i>Nummulites fabianii</i> , <i>N. ex. gr. fabianii</i> , <i>N. perforatus</i> , <i>N. striatus</i> , <i>Assilina spira</i> , <i>Asterigerina rotula</i> , <i>Fabianii cassis</i> , <i>Chapmanina gassinensis</i> , <i>Linderina brugesii</i> , <i>Eorupertia magna</i> , <i>Halkyardia minima</i> , <i>Alveolina fusiformis</i> , <i>A. elongata</i> , <i>Praerhapydionina huberi</i> .	Upper Lutetian-Priabonian
Avşar, 1996	<i>Nummulites striatus</i> , <i>Asterigerina rotula</i> , <i>Gyroidinella magna</i> , <i>Halkyardia minima</i> , <i>Praebullalveolina afyonica</i> , <i>Praerhapydionina huberi</i> , <i>Peneroplis damesini</i> , <i>P. aff. laevigatus</i> , <i>Spirolina aff. cylindracea</i> , <i>Miliolidae</i> .	Upper Lutetian-Priabonian
Özcan et al., 2019a	<i>Discocyclina pratti</i> , <i>D. trabayensis</i> , <i>D. augustae</i> , <i>D. radians</i> , <i>D. euaensis</i> , <i>D. dispansa</i> , <i>D. pulcra</i> , <i>D. discus</i> , <i>Nemkovella evae</i> , <i>N. strophiolata</i> , <i>N. daguini</i> , <i>Orbitoclypeus douvillei</i> , <i>O. haynesi</i> , <i>O. varians</i> , <i>O. zitteli</i> , <i>Orbitoclypeus n. sp. A</i> , <i>Asterocyclina stellata</i> , <i>A. stella</i> , <i>A. sireli</i> , <i>A. kecskemetti</i> , <i>A. alticostata</i> , <i>Nummulites garganicus</i> , <i>N. hormoensis</i> , <i>N. perforatus</i> , <i>N. maximus</i> , <i>N. gizehensis</i> , <i>N. ptukhiani</i> , <i>N. striatus</i> , <i>N. biarrizensis</i> , <i>N. anomalus</i> , <i>Heterostegina armenica</i> , <i>Operculina ex. gr. gomezi</i> , <i>Assilina schwageri</i> , <i>A. exponens</i> , <i>Sphaerogypsina globulus</i> , <i>Asterigerina rotula</i> , <i>Fabiania cassis</i> , <i>Chapmanina gassinensis</i> , <i>Silvestriella tetraedra</i> , <i>Gyroidinella sp.</i> , <i>Calcarina sp.</i> , <i>Linderina sp.</i>	Bartonian-lower Priabonian
Present study	<i>Nummulites hormoensis</i> , <i>N. cf. hormoensis</i> , <i>N. fabianii</i> , <i>N. cf. fabianii</i> , <i>N. ex. interc. hormoensis-fabianii</i> , <i>N. striatus</i> , <i>Operculina ex. gr. gomezi</i> , <i>Sphaerogypsina globulus</i> , <i>Asterigerina rotula</i> , <i>Gyroidinella magna</i> , <i>Halkyardia minima</i> , <i>Chapmanina gassinensis</i> , <i>C. elongata</i> , <i>Silvestriella tetraedra</i> , <i>Penarchaias glynnjonesi</i> , <i>Nummulites sp.</i> , <i>Gypsina sp.</i> , <i>Linderina sp.</i> , <i>Planorbulina sp.</i> , <i>Peneroplis sp.</i> , <i>Spirolina sp.</i> , <i>Stomatobinid forms</i> , <i>Rotaliids</i> , <i>Textulariids</i> , <i>Miliolidae</i> .	Upper Bartonian-Priabonian

biometric analysis of reticulate *Nummulites* and determinations of other LBF in this unit.

## 2. Geological setting

The study area is located 15 km northwest of Elazığ, eastern Anatolia, Turkey (Figure 1). Magmatic, metamorphic, and sedimentary units ranging from Devonian–Jurassic to Plio-Quaternary in age crop out in this area and its vicinity (Figures 1B, 1C, and 2A).

The Kırkgeçit basin which is located on the eastern Taurides (Turkey) was developed in back-arc setting during the closure of the southern branch of Neotethys, situated between Arabian and Anatolian plates, in relation to plate convergence in the Paleogene (Figures 1A and 2B). Metamorphic, magmatic, and sedimentary units of Devonian–Jurassic to late Paleocene in age form the basement of this NE-SW trending basin (Figures 1B, 1C, and 2A). The Devonian–Jurassic-aged Keban metamorphites outcropping in the eastern Taurides is an allochthonous unit and was metamorphized during the late Cretaceous under the amphibolite-greenschist facies conditions in relation with the closure of Neotethys Ocean. The unit consists of regionally metamorphosed rocks such as marble, crystallized limestone, metaconglomerate, calcschist, phyllite-chlorite-sericiteschist (Kaya, 2016). This unit was thrust onto the upper Cretaceous Elazığ magmatites and the Kırkgeçit Formation in the study area as a result of regional geodynamic evolution in the latest Cretaceous and middle Miocene (Figure 1C). Elazığ magmatites is product of a magmatic arc associated with the subduction resulted with the closure of southern branch of the Neotethys Ocean located between Arabian and Eurasian plates during late Cretaceous. This unit comprises volcanic, subvolcanic, and plutonic rocks in the Elazığ region (Beyarslan and Bingöl, 2018). The middle-upper Eocene

Kırkgeçit Formation, the fossil content of which is the subject of this study, was deposited in a block-faulted basin formed on a back-arc setting under an extensional regime (Cronin et al., 2000b; Aksoy et al., 2005). The Kırkgeçit Formation rests unconformably on the older units such as the Keban metamorphites and the Elazığ magmatites. The facies characteristics of Kırkgeçit Formation indicate that the deposition environment of the unit had highly irregular basin floor topography. In the following paragraphs, more detailed information has been given about the lithology and fossil content of the unit. The upper Miocene–early Pliocene-aged Karabakır Formation (also known as Çaybağı Formation) unconformably overlies the older units and is represented by red-gray conglomerate, sandstone, siltstone, mudstone, peat, marl, and limestone deposited in a continental environment (Taşgın Koç et al., 2012). These sedimentary rocks have lateral and vertical relationship with volcanic tuffs, ignimbrite and lava flows having an age range of 4.1 to 1.7 Ma in the Elazığ region (Di Giuseppe et al., 2017). Seyrek et al. (2008) also proposed similar age range for the same basaltic rocks occurring over the Kırkgeçit Formation and the Pliocene clastic rocks in the study area (Figures 1B and 1C).

The type locality of the Kırkgeçit Formation is near the Kırkgeçit village located near Van, a city in the eastern Turkey, and it was named by Turkish Petroleum Company (TPAO) geologists (after Perinçek, 1979). It has widespread exposures in an area extending from Elazığ to Van on the eastern Taurides. The formation also crops out in a large area in the vicinity of Elazığ (Figure 1B). The Kırkgeçit basin around Elazığ has approximately E–W direction, and its northern and southern margins were bounded by gravity faults. The Kırkgeçit basin has been considered to be developed under an extensional regime in relation with the geodynamic evolution of southern branch of the Neotethys

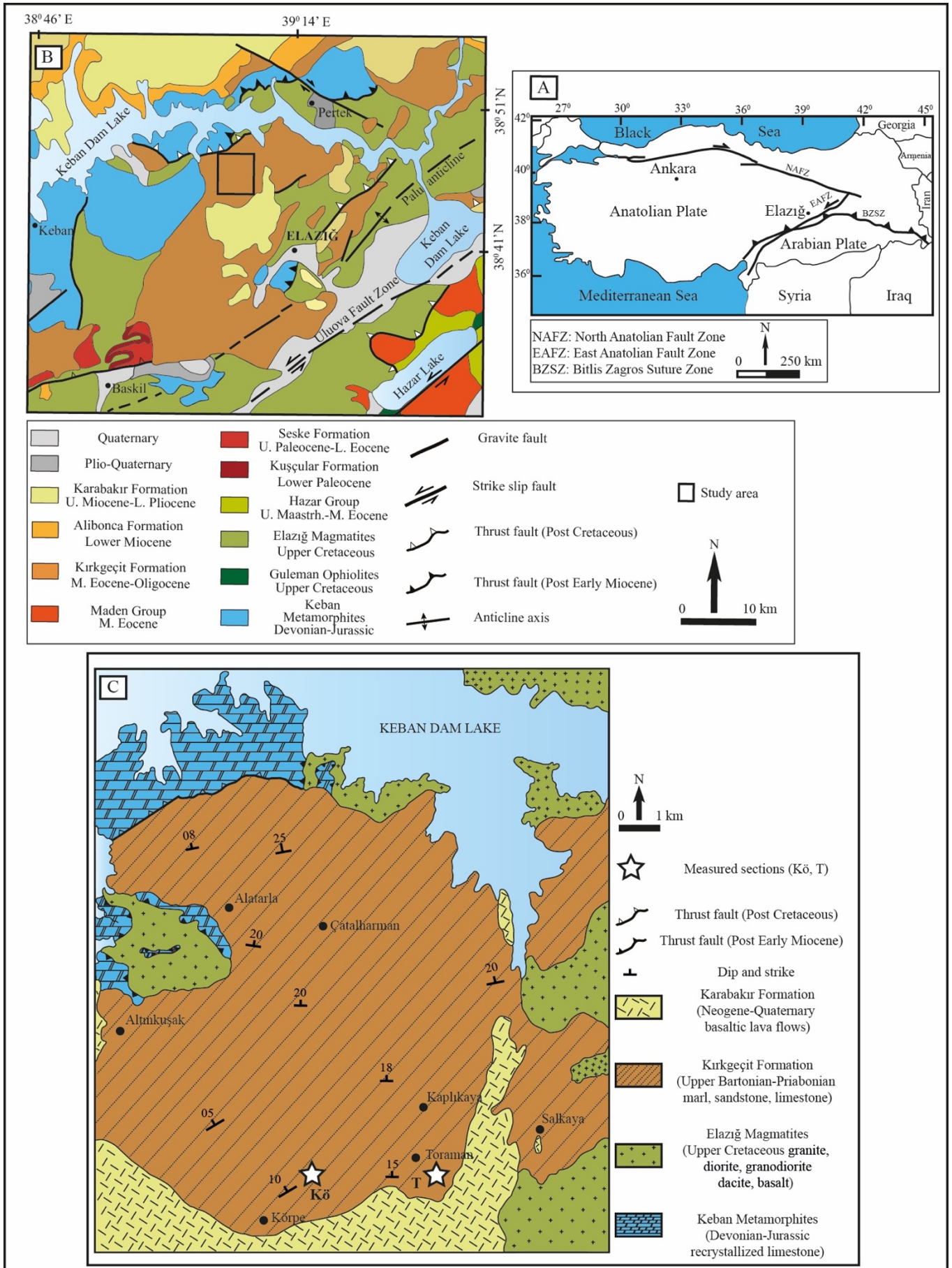


**Figure 1.** (A) The simplified map of Turkey. (B) Geological map of the study area (modified from Aksoy et al., 2005). (C) Geological map of the study area (modified from Avcı, 1983) and location of the measured sections.

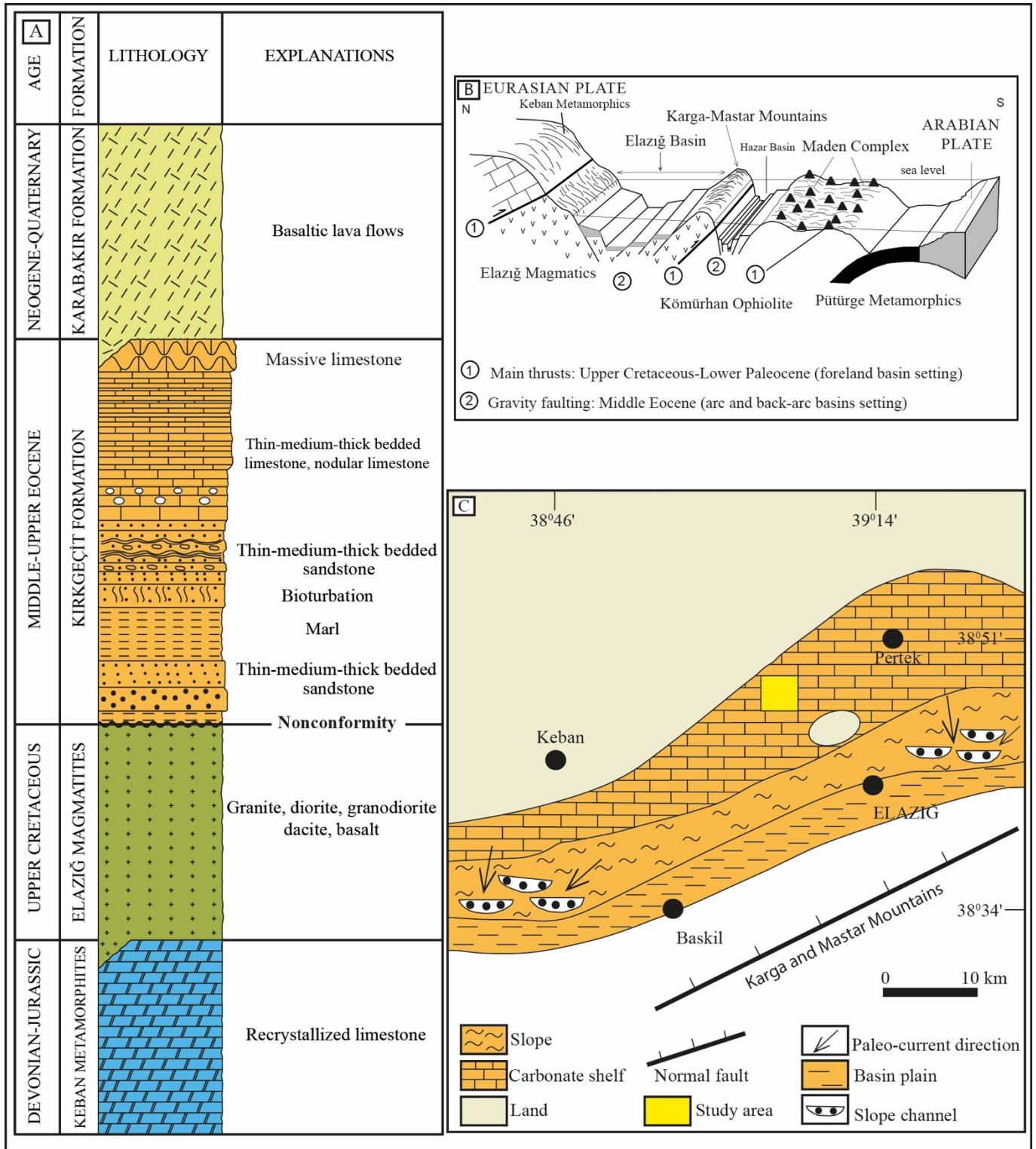


**Figure 2.** (A) Generalized stratigraphy of the study area. (B) Cartoon showing the paleogeography of the Kirkgeçit Formation in the middle Eocene (Özkul, 1988; Cronin et al., 2000a). (C) Paleogeographic map of the region during the middle-late Eocene (Aksoy et al., 2005).

Ocean located between Anatolian and Arabian plates (Figure 2B) (Aksoy et al., 2005). The sediments of the Kirkgeçit Formation deposited in the deep-water and shelfal environments are related with rapid basin subsidence controlled by block-faults forming the basin (Özkul and

Kerey, 1996; Cronin et al., 2000b) (Figure 2B). Along the northern margin of the Kirkgeçit basin, shallow marine facies (i.e. tidal flat and stormy shelf complex deposits) were deposited (Türkmen et al., 2001), by contrast, towards the south to southwest, deep water siliciclastics are dominant (Özkul, 1988; Özkul and Kerey, 1996; Cronin et al., 2000a, b)

(Figure 2C). Özcan et al. (2019a) stated that the depositional environment of the Bartonian–early Priabonian Kırkgeçit Formation in the Baskil area (westward from Elazığ) ranges from shelf to basin plain. Özcan et al. (2006, 2019a) have presented the Bartonian LBF content of Kırkgeçit Formation in the Baskil region in detail.

### 3. Materials and methods

The benthic foraminiferal assemblage of the Kırkgeçit Formation was collected from Körpe and Toraman measured sections (Figure 1C). Their thicknesses are 144 m and 146 m, respectively. In order to define biozones based on LBF, 289 oriented thin sections (169 samples of reticulate *Nummulites* (Table 2), 83 samples of other *Nummulites*, 37 samples of *Operculina* ex.gr. *gomezi*) from loose samples, and 50 thin sections from rock samples were prepared. These are

determined from the equatorial and axial thin sections of loose and rock samples collected along the measured sections. For biometry, 169 tests of megalospheric form of reticulate *Nummulites*, collected from two measured sections as named Körpe (36 samples) and Toraman (133 samples), were used (Table 2).

Shallow benthic foraminiferal biozones were determined based on studies by Serra-Kiel et al. (1998), Less and Özcan (2012), and Papazzoni et al. (2017). For the textural classifications of carbonates, Dunham (1962) classification was followed, while the paleoenvironmental interpretations were based on Hottinger (1997), Beavington-Penney and Racey (2004), Flügel (2004), and Nebelsick et al. (2005).

In this study, 11 parameters, which are listed in Figure 3 and Table 2, were measured on the species discrimination of reticulate *Nummulites* following the works of Schaub (1981),

**Table 2.** Biometry of reticulate *Nummulites*.

Loose Samples	No	Prange (µm) Pmean (µm)± s.e)	r (µm)	r1 (µm)	r2 (µm)	r3 (µm)	LL (µm)	HL (µm)	D2 (µm)	D3 (µm)	N	E	Taxon/SBZ
Kö6, Kö7	21	134–265 200 ± 7.99	169–284	293–449	436–649	646–888	69–285	65–175	764–1476	907–1589	16–22	12–17	<i>N. ex. interc. hormoensis-fabianii</i> SBZ 18
Kö9	1	192 –	206	375	535	751	176–192	96–133	979	1607	27	17	<i>N. cf. hormoensis</i> SBZ 18
Kö10	2	193–255 224 ± 21.92	220	398	549	759	112–286	107–170	980	1346	–	13	<i>N. cf. fabianii</i> SBZ 19-20
Kö11	9	178–356 262 ± 16.57	258–353	422–655	549–833	700–957	69–295	61–202	1010–1345	1341–1667	16–19	16–18	<i>N. fabianii</i> SBZ 19-20
Kö14	3	241–326 270 ± 23	316–363	493–508	659–673	778–906	116–339	63–142	1140–1218	1391–1602	18	15	<i>N. fabianii</i> SBZ 19-20
T3	16	127–230 168 ± 7.64	160–280	285–440	420–630	640–800	70–220	80–150	700–1300	890–1400	15–20	11–17	<i>N. hormoensis</i> SBZ 18
T6a	13	190–369 300 ± 14.12	243–361	457–590	645–838	787–1108	111–385	99–187	1134–1497	1465–2052	19–20	17–18	<i>N. fabianii</i> SBZ 19-20
T7, T7a	16	250–359 309 ± 8.36	80–391	463–637	649–887	814–1166	58–364	89–224	1144–1560	1441–2091	17–24	16–21	<i>N. fabianii</i> SBZ 19-20
T8, T8a	29	195–404 289 ± 9.10	212–381	413–609	583–815	718–1079	74–339	62–207	1043–1496	1332–1986	13–26	11–21	<i>N. fabianii</i> SBZ 19-20
T9	32	187–368 283 ± 7.75	242–394	416–577	618–765	751–981	79–330	90–201	1145–1391	1520–1845	18–27	15–23	<i>N. fabianii</i> SBZ 19-20
T10	27	185–397 297 ± 9.60	216–389	316–571	226–783	733–1054	74–336	70–203	1130–1520	1340–2045	17–21	16–20	<i>N. fabianii</i> SBZ 19-20

P (µm): The inner cross diameter of the proloculus (range and mean ± standard error (s.e)), r (µm): Distance from center of proloculus to edge of deuteroeculus (range), r1 (µm): Radius of the 1st whorl (range), r2 (µm): Radius of the 2nd whorl (range), r3 (µm): Radius of the 3rd whorl (range), LL (µm): The inner length of the chamber in 3rd whorl (range), HL (µm): The inner height of the chamber in 3rd whorl (range), D2 (µm): Diameter of 1st and 2nd whorls (range), D3 (µm): Diameter of successive 3rd whorl (range), N: Number of chambers in the 1st and 2nd whorls (range), E: Number of chambers in the 3rd whorl (range).

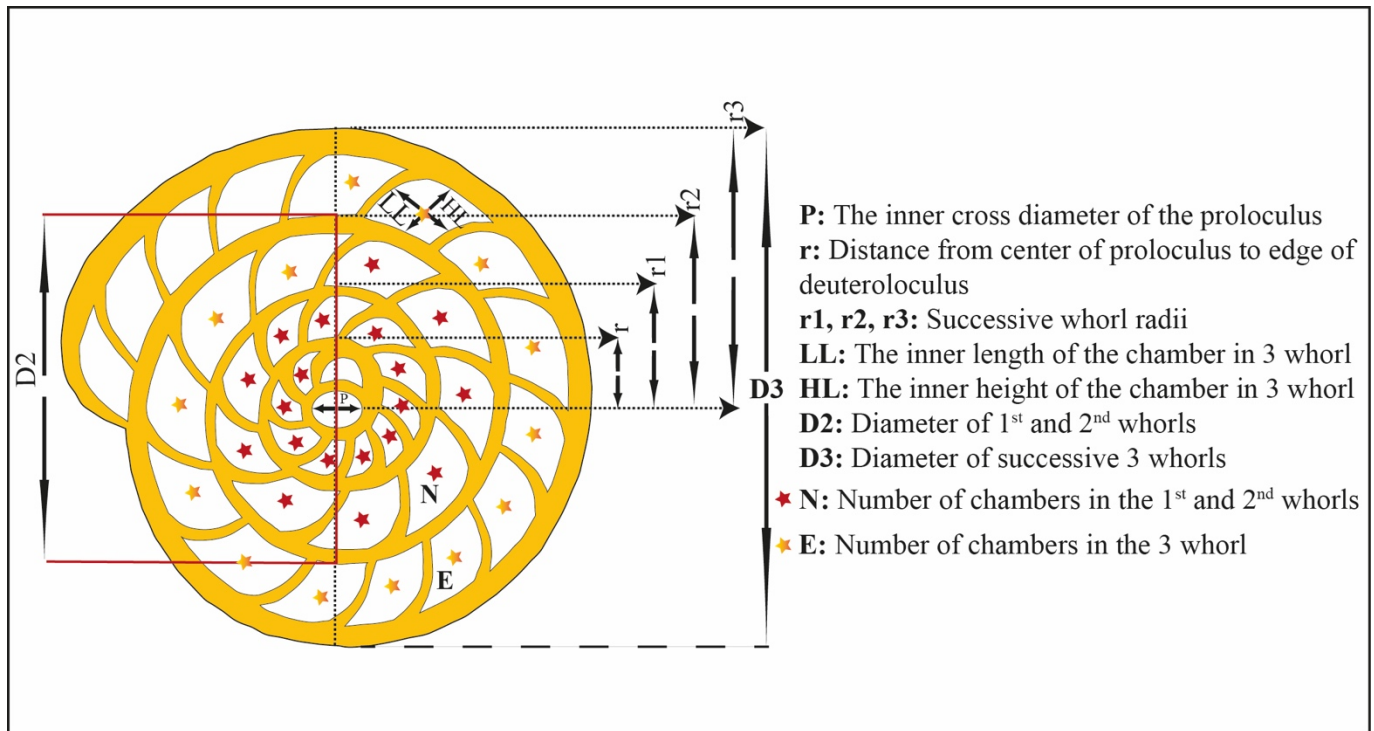


**Figure 3.** Schematic section of *Nummulites* to illustrate biometric measurements carried out in this study (modified from Saraswati et al., 2017).

Racey (1995), Papazzoni (1998), Cotton et al. (2015), Saraswati et al. (2017), and Özcan et al. (2019b). The classification of reticulate *Nummulites* was made by using the criteria given in Özcan et al. (2019b).

#### 4. Description of measured sections

Two stratigraphic sections named as Körpe and Toraman, were measured in the latest Bartonian–Priabonian aged Kirkgeçit Formation.

##### 4.1. Körpe section (Kö)

The section (base of the section: 38°45'24.75"N, 39°8'17.96"E, top of the section: 38°45'36.85"N, 39°8'17.71"E) is 144 m thick, and was taken through the latest Bartonian–Priabonian Kirkgeçit Formation (Figure 1C).

The base of this section is represented by layers ranging from thin (1–10 cm) to intermediate (10–20 cm) bedded yellowish-green fine to medium grained sandstone having marl intercalations, includes bioturbation, and is dominated by reworked and oriented *Nummulites* (Figures 4 and 5).

The middle and upper part of this section is characterized by thin (1–10 cm) to medium (10–30 cm)/thick (30–80 cm) bedded and massive (1–2.5 m) yellowish-beige limestone and the middle part of the section is dominated by *Nummulites* (Figures 4 and 5).

##### 4.2. Toraman section (T)

The section (base of the section: 38°46'5.85"N, 39°10'23.59"E, top of the section: 38°46'13.54"N, 39°10'20.53"E) has a thickness of 146 m and was taken through the latest Bartonian–Priabonian Kirkgeçit Formation (Figure 1C).

The base of this section is represented by thin (1–10 cm), medium (10–30 cm), and thick (30–60 cm) bedded yellowish-green, fine-medium grained sandstone, includes

bioturbation, and is dominated by reworked and oriented *Nummulites* (Figures 6 and 7).

The middle and upper parts of this section comprise thin (1–10 cm), medium (10–30 cm), thick (30–60 cm) bedded and massive (4–5 m) yellowish-beige limestone. The middle part of the section is dominated by *Nummulites* (Figures 6 and 7).

#### 4.3. The facies and depositional environment

Nine facies types have been determined in the studied samples based on the depositional texture and fossil content (Figures 5, 7, and 8). These are facies 1, *Nummulites* sandstone (locally marl/siltstone); facies 2, *Nummulites* grainstone; facies 3, *Nummulites* packstone-grainstone; facies 4, *Nummulites* wackestone; facies 5, *Nummulites* wackestone-packstone; facies 6, boundstone; facies 7, porcellaneous foraminifera grainstone; facies 8, porcellaneous foraminifera packstone; facies 9, porcellaneous foraminifera packstone-grainstone. Facies bearing LBF are considered to be deposited in a relatively shallow water environment (carbonate ramp). Facies 1, 2, 3, 4, and 5 are interpreted as deposits on the middle ramp (2a-2b), while facies 6, 7, 8, and 9 on the inner ramp (1b) (Figures 5, 7, and 8).

#### 5. Systematics and biostratigraphy

In defining of shallow benthic zones (SBZ), the appearance and disappearance of LBF species through the measured sections were used as main criteria (Serra-Kiel et al., 1998; Less and Özcan, 2012). The measured sections are represented by SBZ 18 and SBZ 19-20 (Figures 5 and 7).

**Order: Foraminiferida Eichwald, 1830**

**Family: Nummulitidae de Blainville, 1827**

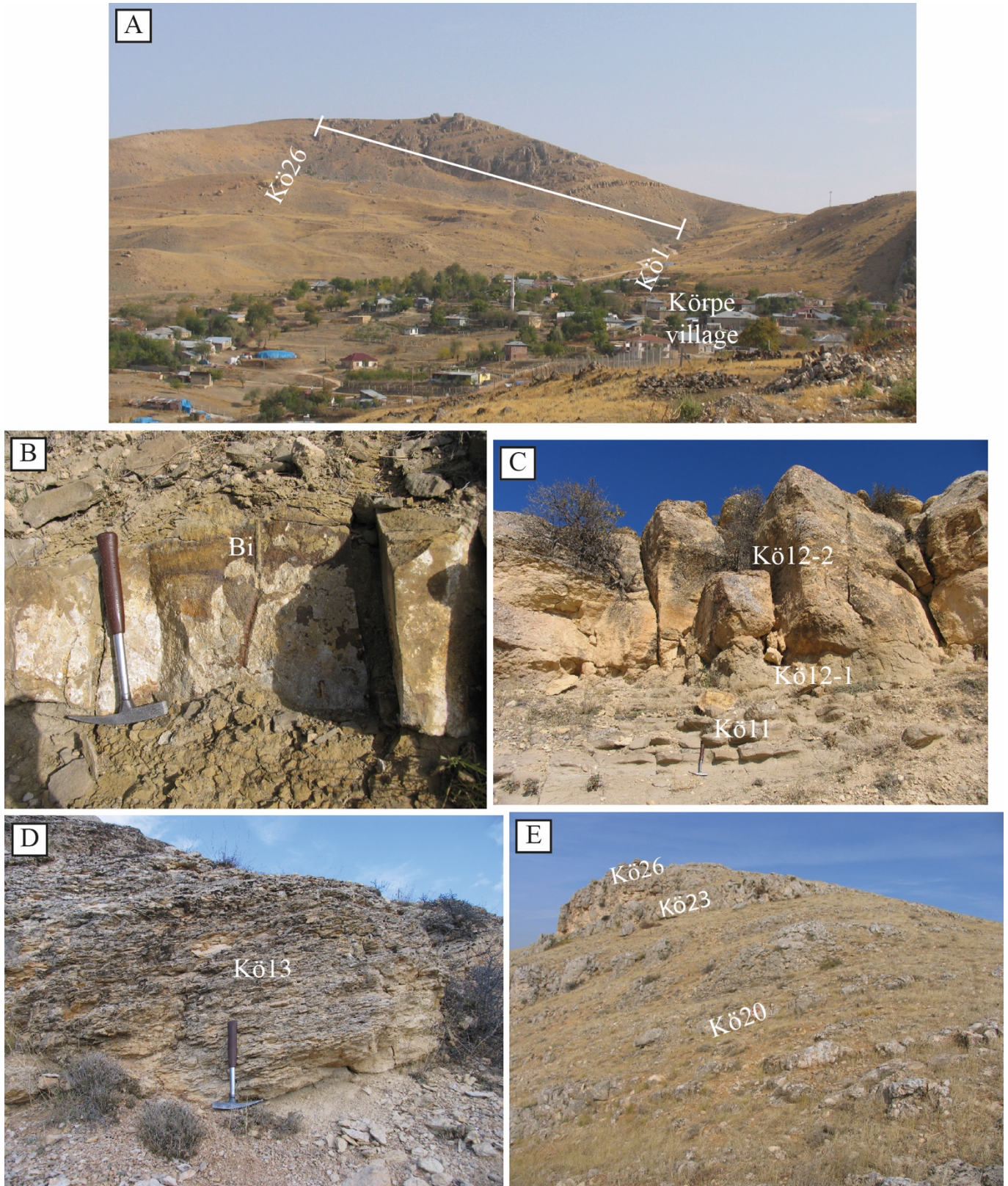


**Figure 4.** Field photographs from the Körpe section. (A) General view of the section. (B) Sandstone with bioturbation (Bi). (C) Sandstone containing marl intercalations. (D) Thin bedded limestone. (E) Medium, thick and massive limestones. Kö1-Kö26: The number of the sample location.

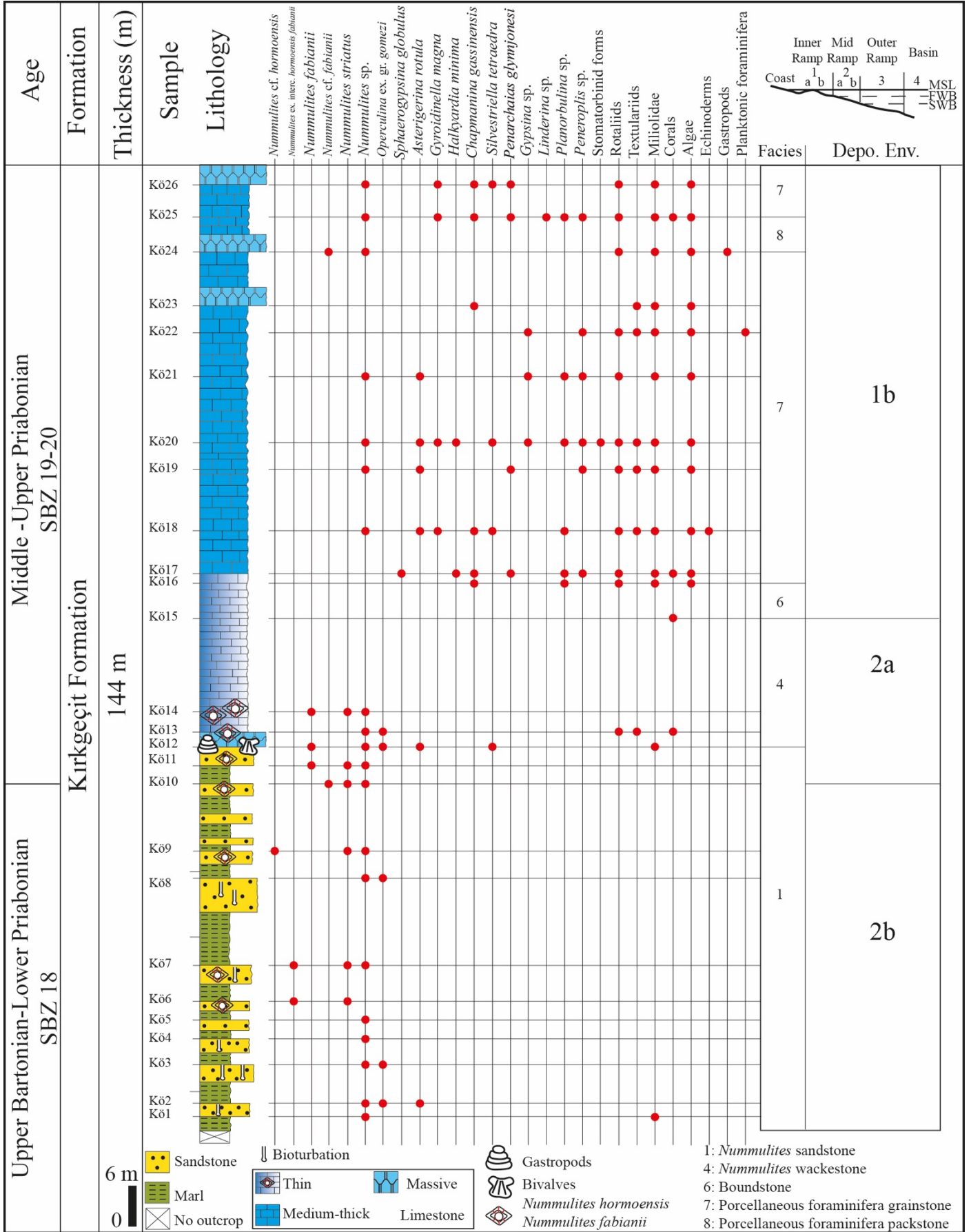
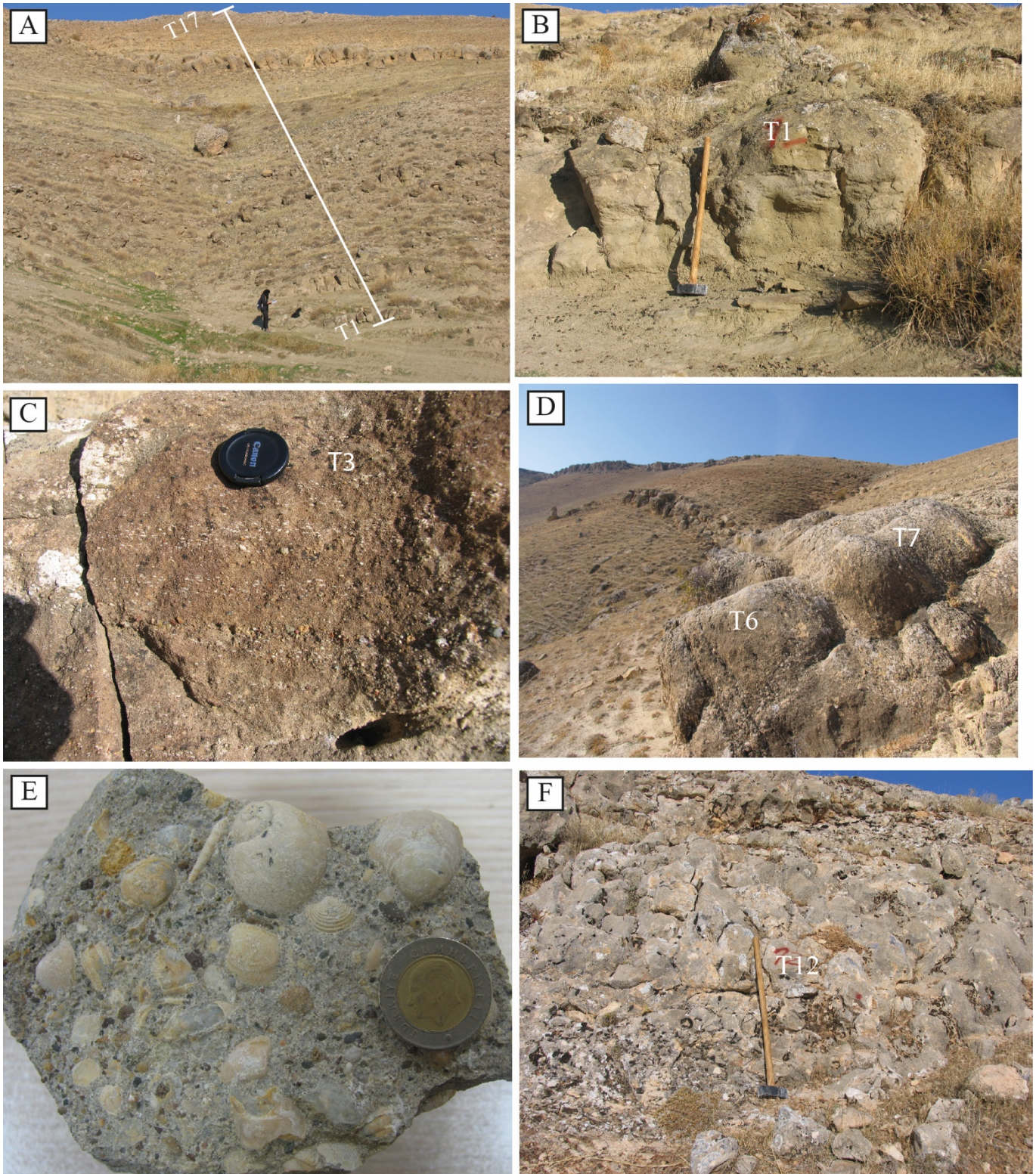


Figure 5. Körpe measured stratigraphic section.





**Figure 6.** Field photographs from the Toraman section. (A) General view of the section. (B) Sandstone beds on the bottom of the section. (C) Sandstone dominated by reworked and oriented *Nummulites*. (D) Limestone dominated *Nummulites*. (E) Sandstone dominated gastropods and bivalves. (F) Thick bedded limestone. T1-T17: The number of the sample location.

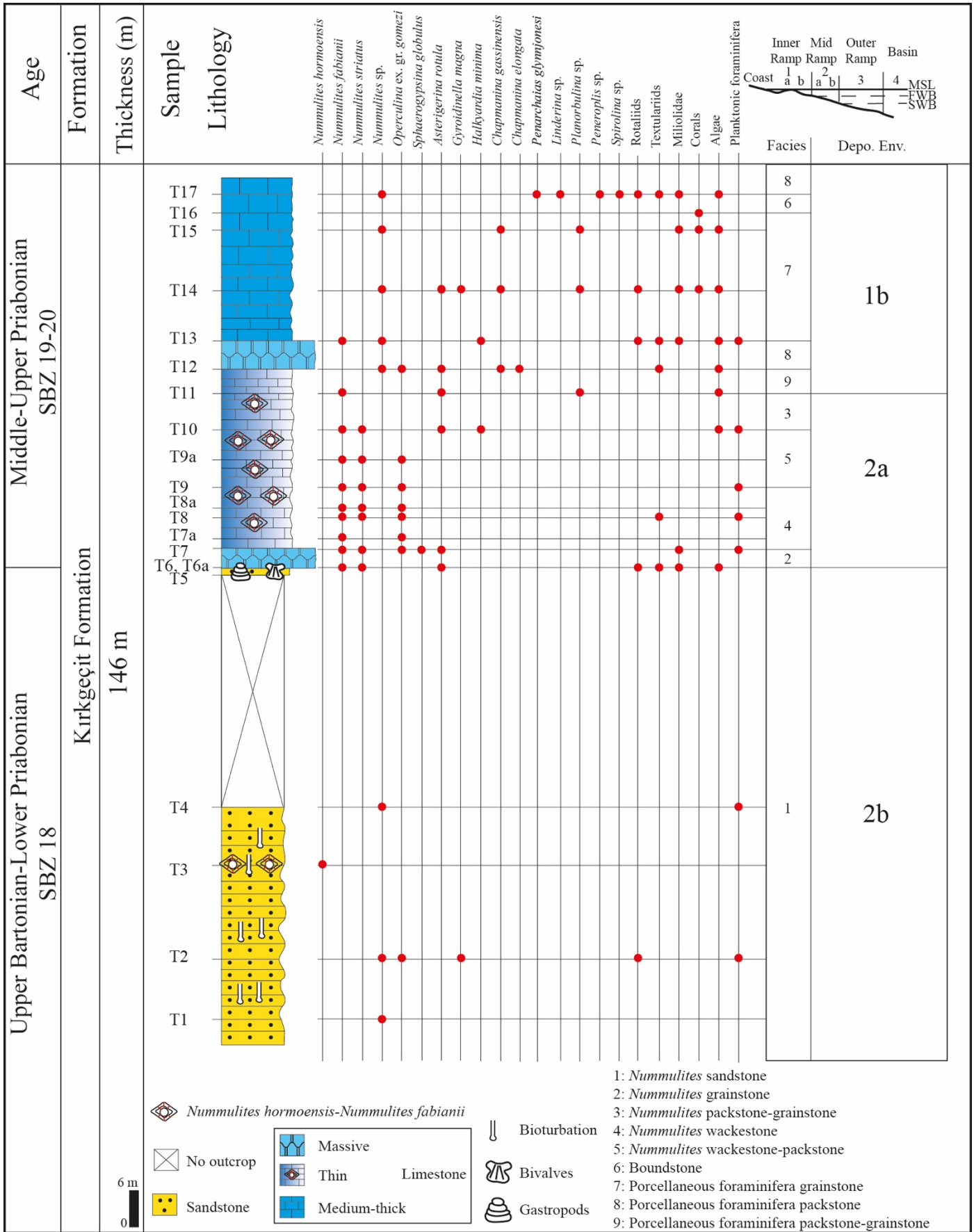
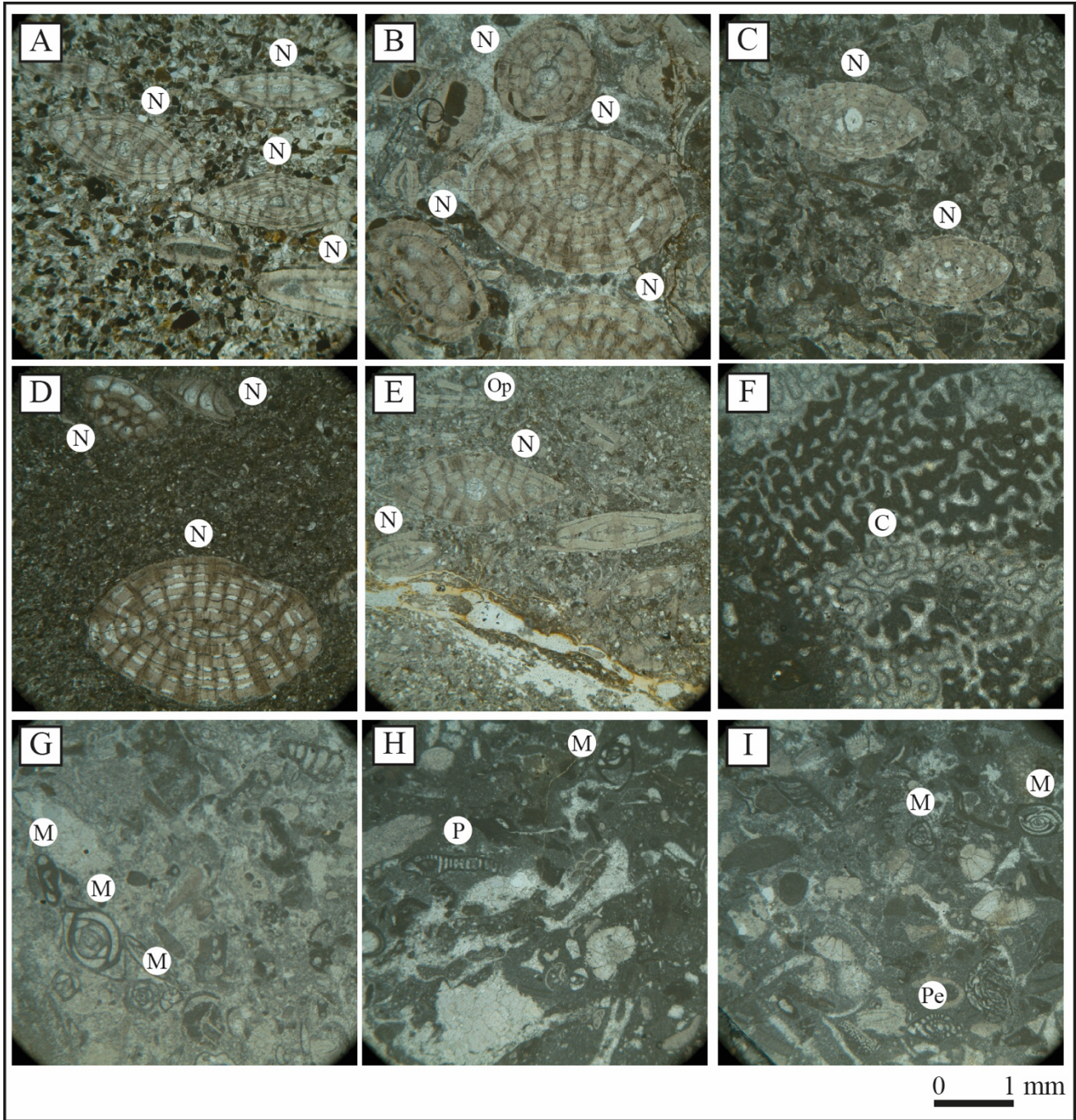


Figure 7. Toraman measured stratigraphic section.



**Figure 8.** Photomicrographs of the facies. (A) *Nummulites* sandstone, sample T3-1-11. (B) *Nummulites* grainstone, sample T6-2-11. (C) *Nummulites* packstone-grainstone, sample T10-4. (D) *Nummulites* wackestone, sample Kö13-15. (E) *Nummulites* wackestone-packstone, sample T9-9. (F) Boundstone, sample Kö15. (G) Porcellaneous foraminifera grainstone, sample Kö22-8. (H, I) Porcellaneous foraminifera packstone, samples, T17-3, T7-15. C: Corals. M: Miliolidae. N: *Nummulites* sp. P: *Peneroplis* sp. Pe: *Penarchaias glynnjonesi*. Op: *Operculina* sp.

### 5.1. Genus: *Nummulites* Lamarck, 1801

*Nummulites* are represented by forms with radiate, reticulate, and granulate types of surface sculpture (so-called morphogroups) (Zakrevskaya et al., 2020). Given the short characteristic of *Nummulites*, supported by measurements of their stratigraphically important parameter, the mean inner diameter of proloculus (Table 2).

The species of *Nummulites* in the studied area were divided into two categories, based on their surface characteristics. *N. hormoensis* and *N. fabianii* belong to the reticulate forms, while *N. striatus* to the radiate forms. Numerous populations from the western Tethys, belonging to the *N. fabianii* lineage, spanning from the late Lutetian to the early Chattian are elaborated (Less et al., 2018; Özcan et al., 2019b). Following

the mean inner cross diameter of the proloculus, “the most important evolutionary parameter” the lineage was subdivided into species (Özcan et al., 2010; Özcan et al., 2019b), among which *N. hormoensis* and *N. fabianii* are present in the study area. The lineage was revised based on the measurement and parameter system mentioned before. Statistically elaborated biometrical data for *N. hormoensis* and *N. fabianii* are summarized in Table 2.

#### 5.1.1. *Nummulites hormoensis* Nuttall & Brighton, 1931 (Figure 9)

1931 *Nummulites hormoensis* n. sp., Nuttall & Brighton, p. 53-54, pl. 3, figs. 1-8.

1998 *Nummulites 'ptukhiani'*, Z.D. Kacharava, Papazzoni, p. 161, 164-165, pl.1, figs.16-24, pl.2, figs.16-21 (with synonymy).

2007 *Nummulites hormoensis* Nuttall & Brighton, Özcan et al., pl. 1, figs. 9, 17.

2010 *Nummulites hormoensis* Nuttall & Brighton, Özcan et al., p. 64, figs. 31h-j.

2019a *Nummulites hormoensis* Nuttall & Brighton, Özcan et al., p. 81, figs.17f-h.

2020 *Nummulites hormoensis* Nuttall & Brighton, Zakrevskaya et al., p.923, figs. 16d-v, 17.

*N. hormoensis* has heavy granules, umbo and reticulation, and most of specimens possess a central boss (a thick granule). The mean inner cross diameter of the proloculus is 140–200  $\mu\text{m}$  (Özcan et al., 2019b).

*N. hormoensis* has mean proloculus size less than 200  $\mu\text{m}$ , although individually this value varies between 115 and 260  $\mu\text{m}$ ; not only the embryo size but also other internal and external features of this species show variations, allowing to distinguish the forms (Zakrevskaya et al., 2020).

The surface of the test is weakly reticulated, it has a central boss and umbo (Figure 9A). Its rounded proloculus is followed by a second chamber, which is gently compressed along the axis of proloculus and following second chamber. Second chamber is either in the same size or slightly smaller than the proloculus (Figures 9B–9F). The diameter of the test varies from 1.30 mm to 3 mm, while the thickness ranges from 0.30 mm to 1.40 mm. The mean diameter and thickness of the test are 2.14 mm and 0.45 mm, respectively. The mean inner cross diameter of the proloculus in the sections ranges between 168  $\mu\text{m}$  and 200  $\mu\text{m}$  (Table 2). Based on the mean inner cross diameter of the proloculus, the specimens from Kö6, Kö7, Kö9, and T3 are assigned to *N. hormoensis*, *N. cf. hormoensis*, and *N. ex. interc. hormoensis fabianii* (Table 2).

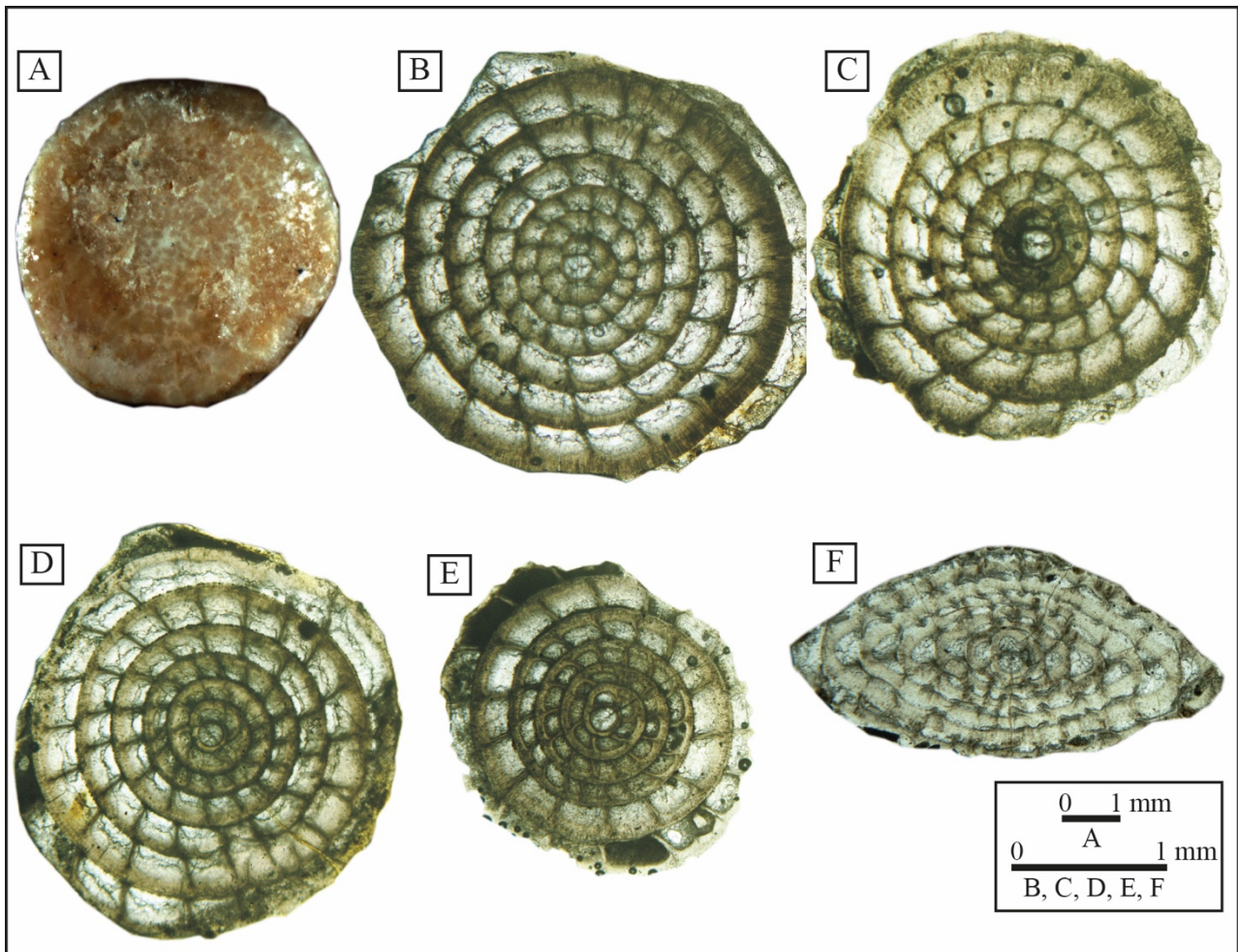


**Figure 9.** Photomicrographs showing *Nummulites hormoensis* (A gen.). (A, B) Samples Kö6-1, (C) Kö7-2, (D) Kö7-8, (E) Kö7-15, (F) T3-1-8. (A) External view. (B–E) Equatorial sections. (F) Axial section.

The stratigraphic range of *N. hormoensis* extends from shallow benthic zone SBZ 18A to SBZ 18C, which are referable to the latest Bartonian and early Priabonian time interval after the modifications of Bartonian–Priabonian boundary with respect to time scale and its reinterpretation by Papazzoni et al. (2017). In this study, the occurrence of these species is

reported as being in the latest Bartonian–early Priabonian (SBZ 18).

5.1.2. *Nummulites fabianii* (Prever in Fabiani, 1905) (Figure 10)

1905 *Brugueirea fabianii* n. sp., Prever in Fabiani, p. 1805, 1811.

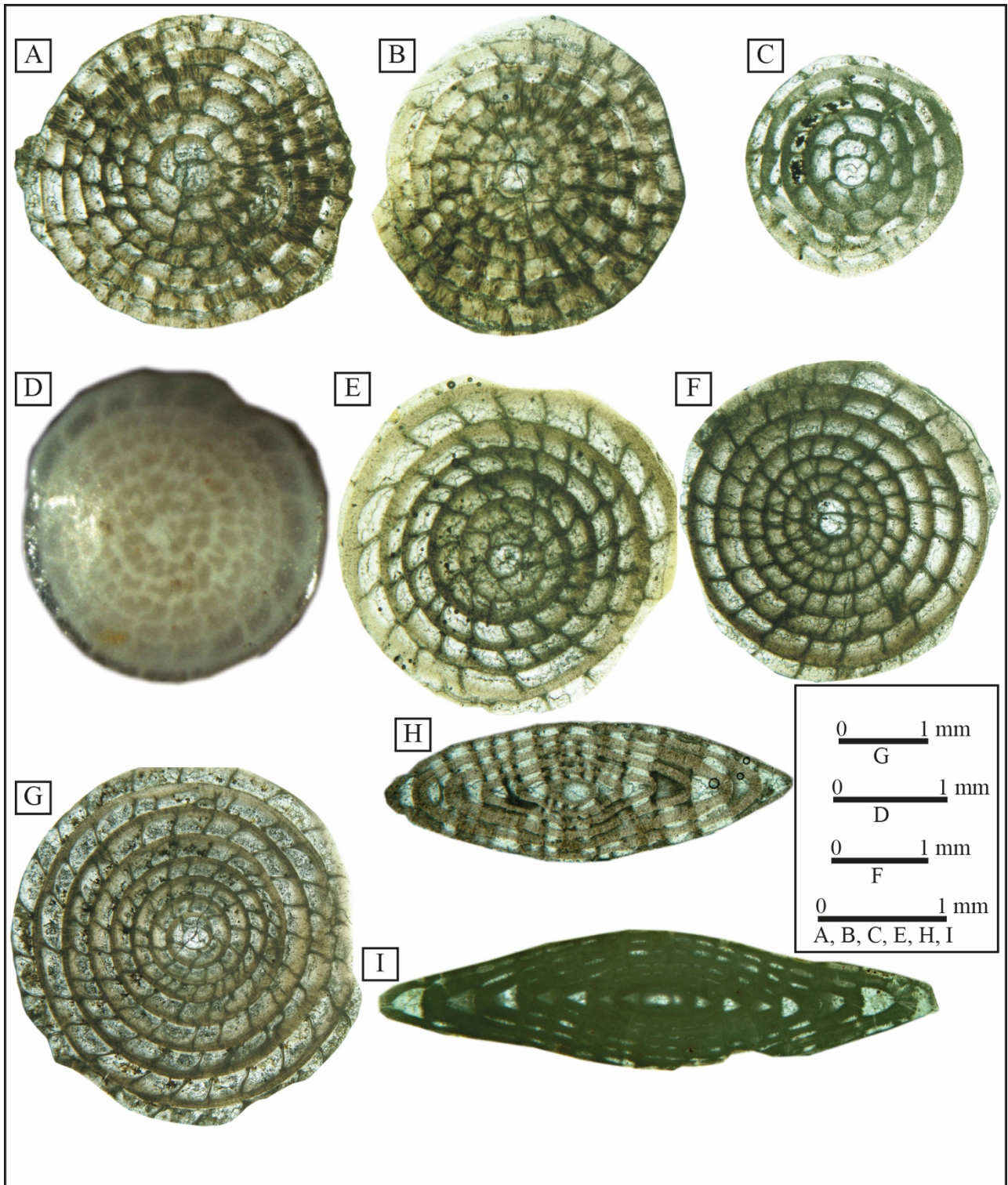


**Figure 10.** Photomicrographs showing *Nummulites fabianii* (A gen.). (A) Samples Kö11-19, (B) T8-25, (C) T8-27, (D, E) T9-22, (F) T9-25, (G) T10-20, (H, I) T8a-10. (D) External view. (A–C, E–G) Equatorial sections. (H, I) Axial sections.

1998 *Nummulites fabianii* (Prever in Fabiani), Papazzoni, p. 165, 168, pl. 1, figs. 1-15, pl. 2, figs. 1-15 (with synonymy).

2010 *Nummulites fabianii* (Prever in Fabiani), Özcan et al., p. 64, figs. 31k-l.

2020 *Nummulites fabianii* (Prever in Fabiani), Zakrevskaya et al., p. 923, 926, figs. 16w-D, 18b, 18c.

*N. fabianii* has weak granules, umbo, and heavy reticulation (Figure 10D). Zakrevskaya et al. (2020) stated that the mean proloculus size of *N. fabianii* is over 200 µm, while Özcan et al. (2019b) suggested that the mean inner cross diameter of the proloculus is in the range of 200 µm to 300 µm.

The surface of the test is heavily reticulated with very weak granulation. It has a central boss (Figure 10D). The diameter of the test varies from 1.20 mm to 5.40 mm, and the thickness from 0.20 mm to 2.10 mm. The mean diameter and thickness of the test are 3.08 mm and 0.82 mm, respectively. The mean inner cross diameter of the proloculus in both sections ranges between 200 µm and 309 µm (Table 2). The mean inner cross proloculus diameter of the specimens from K06, K07, K010, K011, K014, T6a, T7, T7a, T8, T8a, T9, and T10 samples are assigned to *N. fabianii*, *N. cf. fabianii*, and *N. ex. interc. hormoensis fabianii* (Table 2).

The different stratigraphic range of *N. fabianii* from SBZ 19 to SBZ 19-SBZ 21, suggested by different paleontologists, is connected with the different approach (typological, morphometrical) to the *N. fabianii* lineage (Schaub, 1981; Racey, 1994, 1995; Papazzoni, 1998; Serra-Kiel et al., 1998; Özcan et al., 2010, 2019b; Less et al., 2011; Zakrevskaya et al., 2020). The stratigraphic range of *N. fabianii* extends from SBZ 19 to SBZ 21, which is referable to Priabonian to early Rupelian time interval after the modifications of Bartonian–Priabonian boundary with respect to time scale and its reinterpretation by Papazzoni et al. (2017). *N. fabianii* can commonly be found in the sections. Its biostratigraphic range is Priabonian (SBZ 19–20) in this study.

### 5.1.3. *Nummulites striatus* (Bruguière, 1792) (Figure 11)

1792 *Camerina striata* n. sp., Bruguière, p. 399.

1981 *Nummulites striatus* (Bruguière, 1792), Schaub, p. 153-154, pl. 53, figs. 26-31 (with synonymy).

2010 *Nummulites striatus* (Bruguière, 1792), Özcan et al., p. 70, figs. 34h-j.

2019a *Nummulites striatus* (Bruguière, 1792), Özcan et al., p. 84, figs. 19m-p.

2020 *Nummulites striatus* (Bruguière, 1792), Zakrevskaya et al., p. 920, figs. 15c, 15e, 15j.

Zakrevskaya et al. (2020) stated that its surface is covered by radial straight septal traces usually with much expressed trabecules. They also expressed that the tight spire, slightly curved, densely spaced septa are the inner feature of this species, and the proloculus size is 200–400 µm.

A marked trend cannot be observed in the "P" parameter ranging from 180 µm to 360 µm along the sections. This taxon characterizes the zones of SBZ 18 and also SBZ 19A according to Schaub (1981), Serra-Kiel et al. (1998), and Özcan et al. (2019a). Zakrevskaya et al. (2020), in Armenia, argued that contrary to Turkey this species reaches the SBZ 20 biozone.

The surface of *N. striatus* in this study, is covered by radial straight septal traces and it has tight spire, slightly curved, densely spaced septa and mean inner cross proloculus diameter of 198 µm (Figure 11). It is found in the latest Bartonian–Priabonian (SBZ 18–SBZ 19–20).

### 5.2. Genus *Operculina* d'Orbigny, 1826

### *Operculina* ex. gr. *gomezi* Colom & Bauzá, 1950 (Figures 12A and 12B)

2010 *Operculina* ex. gr. *gomezi* Colom & Bauzá, Özcan et al., p. 66, fig. 32x.

2019a *Operculina* ex. gr. *gomezi* Colom & Bauzá, Özcan et al., p. 86, figs. 20d, e.

2020 *Operculina* ex. gr. *gomezi* Colom & Bauzá, Zakrevskaya et al., p. 927, figs. 19d-l.

This genus with folded septa intersected by stolons is represented by the involute *O. ex. gr. gomezi* Colom & Bauzá, 1950 in the Eocene. In contrast, it is represented in the Oligocene by the evolute *O. complanata* (Defrance, 1822). While the first of those mentioned was briefly discussed by Özcan et al. (2010) and Yücel et al. (2020), the second one was mentioned by Özcan et al. (2009a, b) and Özcan and Less (2009).

The first appearance of the *O. gomezi* group nearly corresponds to the Lutetian/Bartonian boundary, according to Özcan et al. (2006) and Less and Özcan (2012).

The representatives of the *O. gomezi* group are arranged as a single evolutionary lineage by Hottinger (1977). Although there are no clear delimitations, single evolutionary lineage in this arrangement, starts with *O. bericensis*, followed by *O. roselli* and ending with *O. gomezi*. The name of *O. ex. gr. gomezi* was also applied in this study. For the 37 specimens of this study, the mean inner cross diameter of the proloculus do not show a prominent increasing trend, and range from 50 µm to 162 µm. The mean inner cross diameter of the proloculus of this species in the latest Bartonian–Priabonian in the Körpe and Toraman sections, is determined as 94 µm.

## 6. Results

The fossil assemblages presented in Figures 9–12 from the Kırkgeçit Formation, are indicative of the SBZ 18 and SBZ 19–20 biozones that are of the latest Bartonian–Priabonian age.

In both sections, LBF are dominated by reticulate *Nummulites* (*N. hormoensis* and *N. fabianii*). *N. fabianii* shows a clear increase in proloculus diameter than *N. hormoensis* (Figure 13). This is accepted as an indication of evolution, and discussed in the following chapter. LBF accumulations in the sections represent inner ramp (1b) and mid ramp (2a, 2b) (Figure 14). Facies 1, 2, 3, 4, and 5 are interpreted as deposits on the middle ramp, while facies 6, 7, 8, and 9 on the inner ramps (Figures 5, 7, and 8). A model illustrating the facies distribution and interpretation of depositional environments are given on Figure 14.

## 7. Discussion

Depositional environment's factors such as water depth, pressure, temperature, substrate, salinity, water energy, nutrients, light level, oxygen concentration, and symbiotic relationship between LBF and photosynthetic algae play a characteristic role in the development of foraminiferal shell (Hottinger, 1997, 2000; Racey, 1995, 2001; Papazzoni, 1998; Hohenegger, 2004, 2005; Beavington-Penney and Racey, 2004; Jorry et al., 2006; Briguglio and Hohenegger, 2009; Renema, 2018). Depth is an important and complex gradient in marine environments because it affects even the results of many single factors (Hohenegger, 2000).

Reticulate *Nummulites* are widespread around the Bartonian/Priabonian boundary (Cotton et al., 2017; Özcan et al., 2019b). It is considered that the transition from the

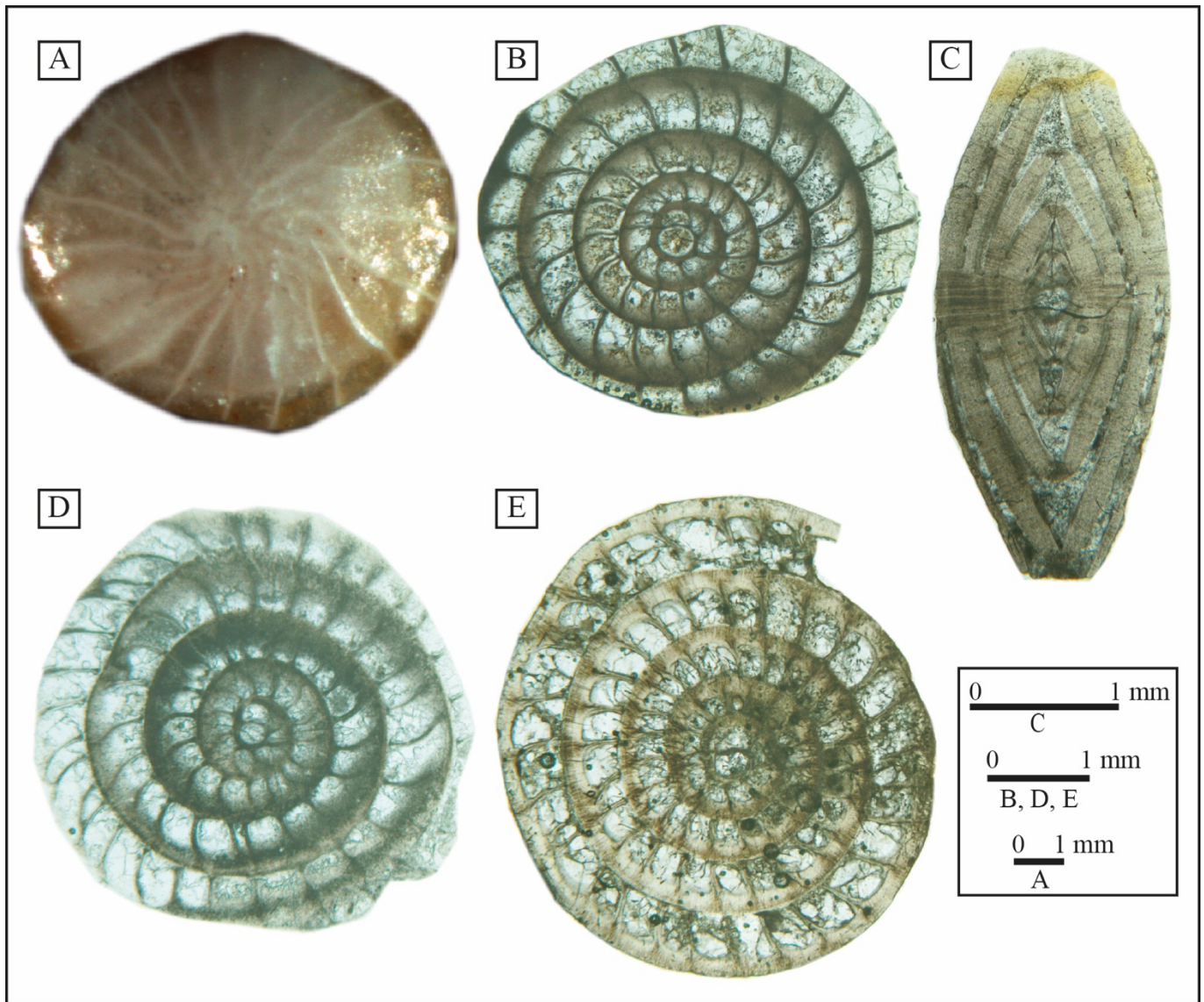


**Figure 11.** Photomicrographs showing *Nummulites striatus* (A gen.). (A, B) Samples T8-9, (C) T8a-9, (D, E) T7-18. (A) External view. (B, D, E) Equatorial sections. (C) Axial section.

Bartonian to the Priabonian corresponds to the extinctions and originations in a lot of microfossil groups. Cotton et al. (2017) suggested that the phylogenetic development of the *N. fabianii* lineage took place in relation with this transition.

Members of the *N. fabianii* lineage are used as indicators of biostratigraphy and evolution depending on their proloculus diameter increasing in time (Schaub, 1981; Papazzoni, 1998; Özcan et al., 2009a, b, 2010; Less and Özcan, 2012; Cotton et al., 2017; Özcan et al., 2019b). However, Drooger (1983) states that irregularities can be seen in the proloculus diameter.

In this study, it has been determined that *N. hormoensis* has small inner cross diameter of proloculus (168–200  $\mu\text{m}$ ), while *N. fabianii* has larger inner cross diameter of proloculus (200–309  $\mu\text{m}$ ) (Table 2). The values of proloculus diameter obtained in this study are in accordance with those obtained from other studies (Table 3).

Foraminifera living in shallow water produce ovate tests with thick walls (Beavington-Penney and Racey, 2004). Such tests provide resistance in turbulent water and prevent protein

damage that can occur due to high light levels. The thinner test walls of species living in deep-water permit more exploitation of the reduced light in such waters, or in shallow water with poor transparency (Drooger, 1983; Beavington-Penney and Racey, 2004). The preparation of Figure 14 was based on these data.

*N. hormoensis* indicates relatively deeper habitat (2b) than *N. fabianii* (2a) (Figure 14). *N. fabianii* has robust test with thick walls, while *N. hormoensis* has elongated test with thinner walls in relation to increasing water depth in generally.

Papazzoni et al. (2017) suggest that the stratigraphic range of *N. hormoensis* extends from SBZ 18A to SBZ 18C, which are referable to the latest Bartonian and early Priabonian time interval after the modifications of Bartonian–Priabonian boundary with respect to time scale and its reinterpretation.

Özcan et al. (2019b) suggested that *N. fabianii* is used as an indicator of Priabonian to early Rupelian.

It is suggested that *Chapmanina gassinensis* (Silvestri) and *Silvestriella tetraedra* (Gümbel) appear first in the lower part of SBZ 18A, close to the Bartonian–Priabonian boundary (Less

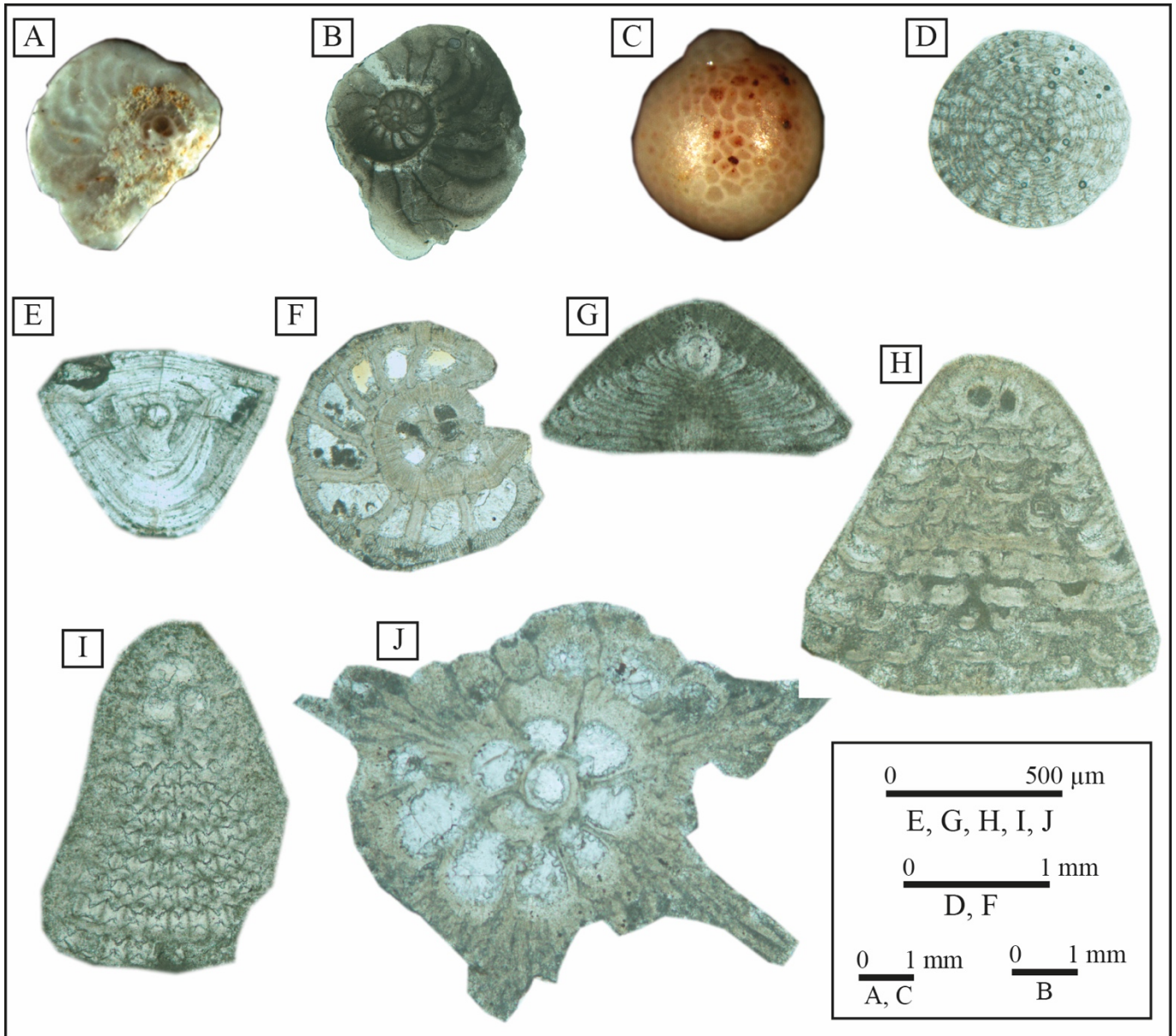


**Figure 12.** Photomicrographs showing larger benthic foraminifera. (A, B) *Operculina* ex. gr. *gomezi*, sample T9-1. (C, D) *Sphaerogypsina globulus*, sample T8-2. (E) *Asterigerina rotula*, sample Kö17-10. (F) *Gyrodinella magna*, sample Kö18-3. (G) *Halkyardia minima*, sample T13-2. (H) *Chapmanina gassinensis*, sample Kö16-8. (I) *Chapmanina elongata*, sample T12. (J) *Silvestriella tetraedra*, sample Kö12-7.

and Özcan, 2012; Özcan et al., 2018; Özcan et al., 2019a, b). The first occurrence of these taxa is important in determining the Bartonian-Priabonian boundary in the stratigraphic column.

Serra-Kiel et al. (1998) argued that the Bartonian/Priabonian boundary coincide with the SBZ 18/SBZ 19 boundary. However, in recent studies, this boundary has been changed by Costa et al. (2013) and Papazzoni et al. (2017) to be within SBZ 18. Followed Less and Özcan (2012) in the assignment of SBZ 18, SBZ 19 to the sections measured from Kirkgeçit Formation. In this study, *N. hormoensis* indicates SBZ 18 while *N. fabianii* represents SBZ 19-20.

The Kirkgeçit Formation in the study area was previously dated as late Lutetian to Priabonian based on LBF (Avşar, 1983, 1991, 1996). In some studies (Özcan et al., 2006, 2019a)

carried out to the west of Elazığ, the presence of fossils indicating Bartonian was mentioned in the outcrops of the same unit. In this study, the Kirkgeçit Formation was dated as latest Bartonian–Priabonian according to the benthic foraminifera content (Table 1).

Eocene sedimentary units, which were deposited in tropical/subtropical shallow-marine environments of Neotethys region, are very rich in nummulitic accumulations (Pleş et al., 2020). These accumulations consist predominantly of packstones, wackestones and grainstones, and microfacies analyses of nummulite accumulations represent inner, mid, and outer ramp in the shelf. Porcellaneous benthic foraminifera are dominated in inner ramp, while hyaline foraminifera are dominated in mid and



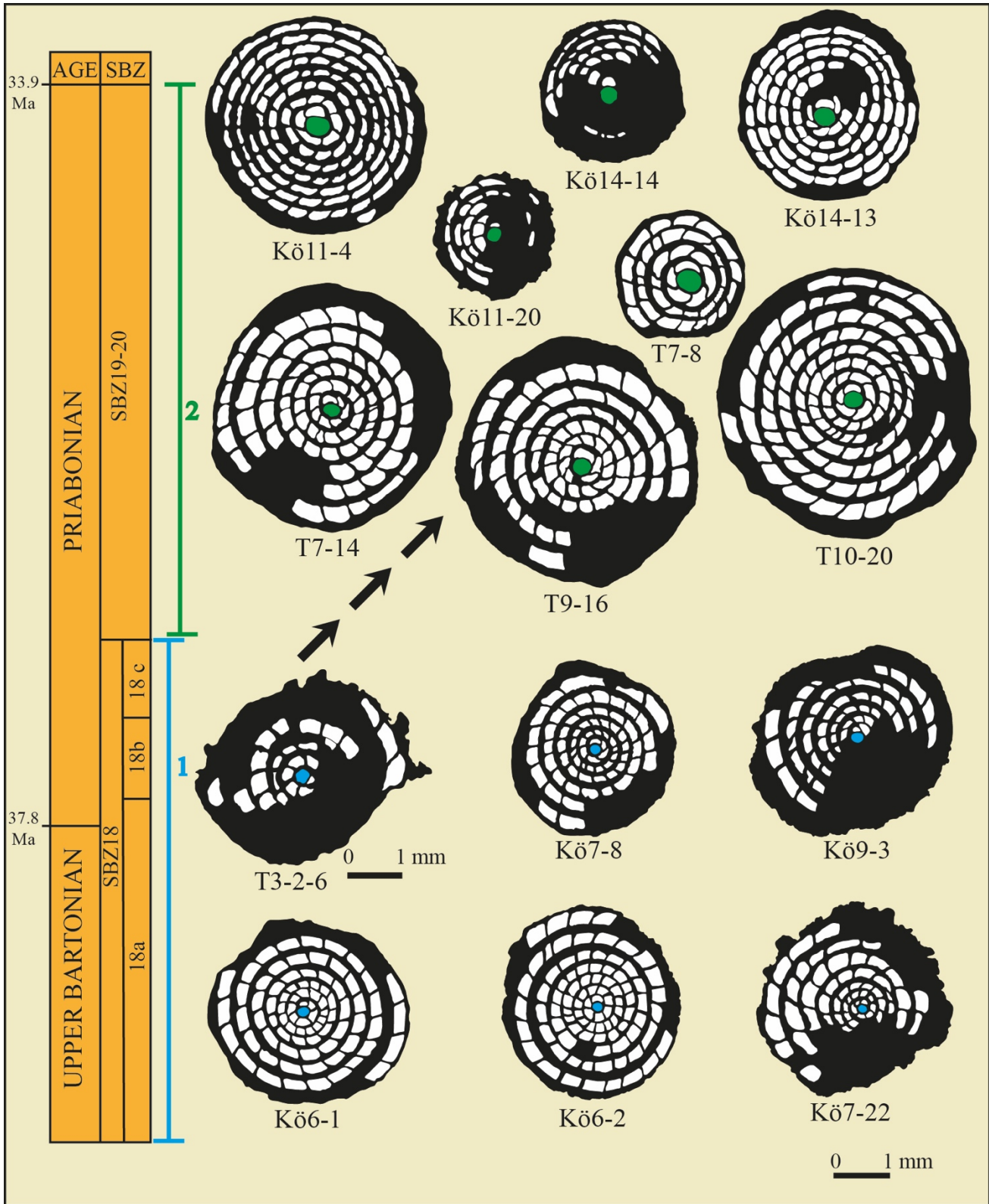


**Figure 13.** The evolutionary scheme of the Kirkgeçit basin late Bartonian-Priabonian reticulate *Nummulites*. SBZ biozones are from Serra-Kiel et al. (1998), subzones (18A, 18B, 18C, 19A, 19B) from Less et al. (2008) and Less and Özcan (2012). T: Toraman and Kö: Körpe sections. Blue embryos in zone 1 indicate SBZ 18, while green embryos in zone 2 indicate SBZ 19-20.

outer ramp (Racey, 2001; Romero et al., 2002; Colombié and Strasser, 2005; Adabi et al., 2008; Banerjee et al., 2018). The coarse environmental generalizations concluded from relative

abundance patterns of fossil LBF give us an idea of relative depth of the depositional environment, but not of absolute depths in meters (Drooger, 1983). In this study, porcellaneous

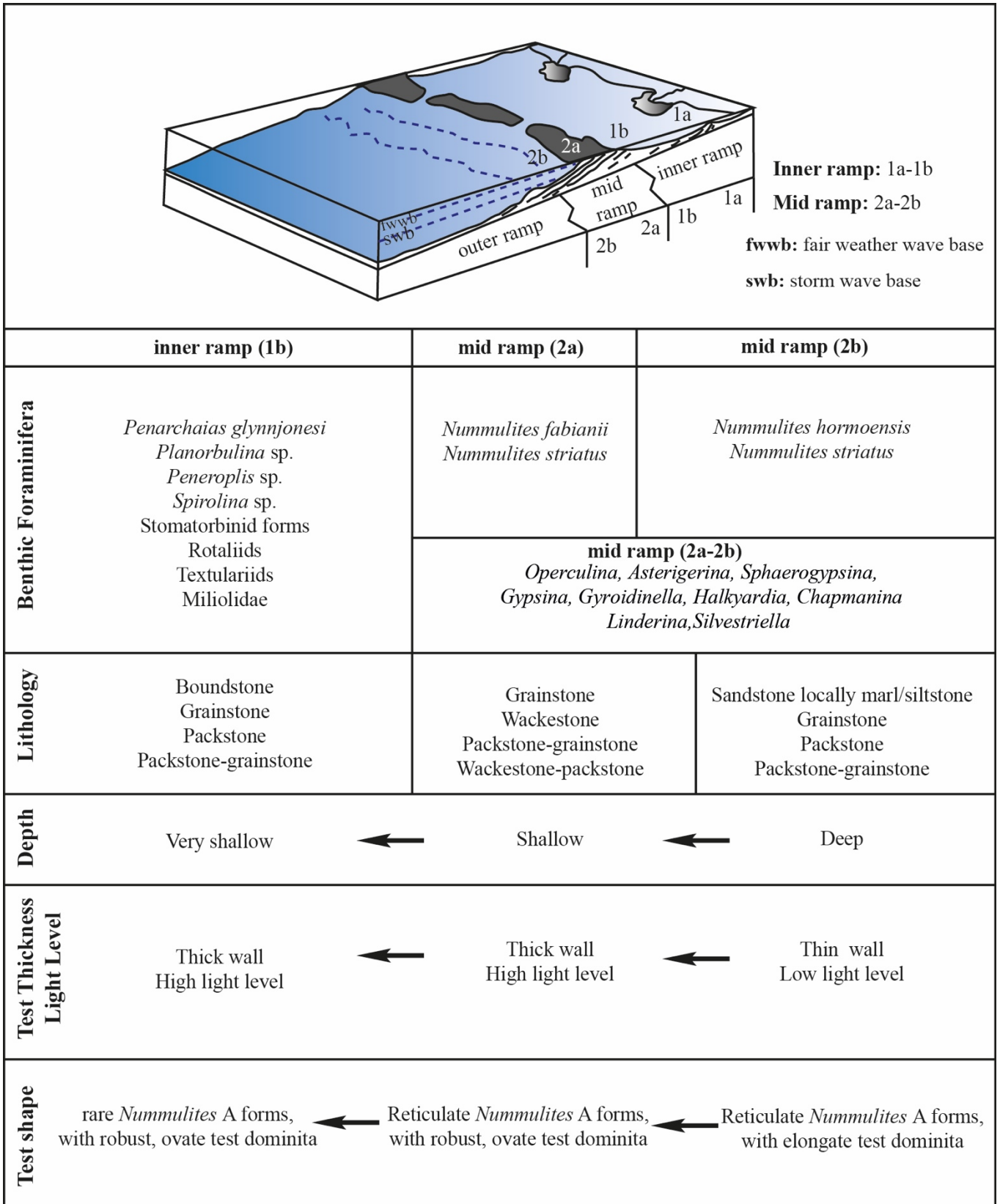


**Figure 14.** Key faunal associations determined from the carbonate ramps of Eocene in the Kırkgeçit basin, summarizing the variation in test shape, light and depth along the paleoenvironmental gradient (modified from Romero et al., 2002 and Beavington-Penney and Racey, 2004).

benthic foraminifera dominated inner ramp (1b) while hyaline foraminifera dominated mid ramp (2a-2b) (Figure 14).

According to Aksoy et al. (2005), shelf carbonates are dominant at the northern part of the Kırkgeçit basin in which the study area is, whereas clastic sedimentary rocks of the

**Table 3.** The comparison of the mean inner cross diameter of the proloculus (Pmean ( $\mu\text{m}$ )) of reticulate *Nummulites* in previous studies and present study.

Taxon	Özcan et al., 2010 Pmean ( $\mu\text{m}$ )	Less et al., 2011 Pmean ( $\mu\text{m}$ )	Özcan et al., 2019a Pmean ( $\mu\text{m}$ )	Özcan et al., 2019b Pmean ( $\mu\text{m}$ )	Zakrevskaya et al., 2020 Pmean ( $\mu\text{m}$ )	Present Study Pmean ( $\mu\text{m}$ )
<i>N. hormoensis</i>	164–195	144–172	150–160	152–153	169	168
<i>N. cf. hormoensis</i>	-	-	-	-	175	192
<i>N. ex. interc. hormoensis fabianii</i>	-	199	-	-	-	200
<i>N. fabianii</i>	210–245	225–304	-	-	242	262–309
<i>N. cf. fabianii</i>	-	-	-	-	-	224

slope environment are widespread in the southern part of the basin. Data obtained from this study is compatible with shallow carbonate deposits on the northern part of the basin.

## 8. Conclusion

The latest Bartonian–Priabonian shallow-marine sequence containing diverse assemblages of LBF have been studied. The assemblages of LBF were determined, and correlated with shallow-marine fauna and biota in the deposits of Tethys.

Nummulitid species especially reticulate *Nummulites* as well as other diagnostic genera, such as *Chapmanina* and *Silvestriella*, were determined in this study. Moreover, the biometric data of the *N. hormoensis* and *N. fabianii* from the latest Bartonian–Priabonian of the Kırkgeçit Formation exposures in the northwest of Elazığ were presented for the first time. The direct superposition of *N. fabianii* on *N. hormoensis* is detected in the study area. The change in embryo size of these reticulate *Nummulites* has been

accepted an important indicator for evolution and biostratigraphy.

Kırkgeçit Formation in the study area was dated as late Lutetian–Priabonian by Avşar (1983, 1991, 1996) using LBF. However, the age of the latest Bartonian–Priabonian has been proposed for the unit based on LBF determined in this study (Table 1). Besides, the depositional environment of the Kırkgeçit Formation in the study area has been interpreted as being the inner (1b) and mid parts (2a-2b) of a shallow ramp (Figure 14) based on the new paleontological and sedimentological findings.

## Acknowledgments

The author is grateful to Prof. Dr. Mehmet Özkul (Pamukkale University) and Prof. Dr. Ercan Aksoy (Fırat University) for their support in the fieldwork. The author would like to thank György Less (Miskolc, Hungary) and Elena Zakrevskaya (Moscow, Russia) for their critical and constructive suggestions in their reviewed.

## References

- Adabi MH, Zohdi A, Ghabeishavi A, Amiri-Bakhtiyar H (2008). Applications of nummulitids and other larger benthic foraminifera in depositional environment and sequence stratigraphy: an example from the Eocene deposits in Zagros Basin, SW Iran. *Facies* 54: 499-512. doi: 10.1007/s10347-008-0151-7
- Aksoy E, Türkmen İ, Turan M (2005). Tectonics and sedimentation in convergent margin basins: an example from the Tertiary Elazığ Basin, Eastern Turkey. *Journal of Asian Earth Sciences* 25: 459-472.
- Avşar N (1983). Elazığ yakın kuzeybatısında stratigrafik ve mikropaleontolojik araştırmalar. PhD, Fırat University, Elazığ, Turkey (in Turkish).
- Avşar N (1991). Presence of *Nummulites fabianii* (Prever) group (*Nummulites* ex. gr. *fabianii*) and associated foraminifera in the Elazığ region. *Bulletin of the Mineral Research and Exploration* 112: 71-76.
- Avşar N (1996). Inner platform sediments with *Praebullalveolina afyonica* Sirel and Acar around Elazığ Region (E. Turkey). *Bulletin of the Mineral Research and Exploration* 118: 9-14.
- Banerjee S, Khanolkar S, Saraswati PK (2018). Facies and depositional settings of the middle Eocene-Oligocene carbonates in Kutch. *Geodinamica Acta* 30 (1): 119-136.
- Beavington-Penney SJ, Racey A (2004). Ecology of extant nummulitids and other larger benthic foraminifera: Applications in palaeoenvironmental analysis. *Earth Science Reviews* 67: 219-265.
- Beyarslan M, Bingöl AF (2018). Zircon U-Pb age and geochemical constraints on the origin and tectonic implications of late Cretaceous intra-oceanic arc magmatism in the Southeast Anatolian Orogenic Belt (SE-Turkey). *Journal of African Earth Sciences* 147: 477-497.
- Briguglio A, Hohenegger J (2009). Nummulitids hydrodynamics: an example using *Nummulites globulus* Leymerie, 1846. *Bollettino della Società Paleontologica Italiana* 48 (2): 105-111.
- Colombié C, Strasser A (2005). Facies, cycles, and controls on the evolution of a keep-up carbonate platform (Kimmeridgian, Swiss Jura). *Sedimentology* 52: 1207-1227. doi: 10.1111/j.1365-3091.2005.00736.x
- Costa E, Garcés M, López-Blanco M, Serra-Kiel J, Bernaola G et al. (2013). The Bartonian–Priabonian marine record of the Eastern South Pyrenean Foreland Basin (NE Spain): A new calibration of the larger foraminifera and calcareous nannofossil biozonation. *Geologica Acta* 11 (2): 177-193. doi: 10.1344/105.000001779
- Cotton LJ, Pearson PN, Renema W (2015). A new Eocene lineage of reticulate *Nummulites* (Foraminifera) from Kilwa district, Tanzania; a place for *Nummulites ptukhiani*? *Journal of Systematic Palaeontology* 14 (7): 569-579. doi: 10.1080/14772019.2015.1079562
- Cotton LJ, Zakrevskaya EY, Van der Boon A, Asatryan G, Hayrapetyan F et al. (2017). Integrated stratigraphy of the Priabonian (upper Eocene) Urtsadzor section, Armenia. *Newsletters on Stratigraphy* 50 (3): 269-295. doi: 10.1127/nos/2016/0313
- Cronin BT, Hartley AJ, Çelik H, Hurst A, Türkmen İ et al. (2000a). Equilibrium profile development in graded deep-water slopes: Eocene, Eastern Turkey. *Journal of the Geological Society* 157: 943-955.

- Cronin BT, Hurst A, Çelik H, Türkmen İ (2000b). Superb exposure of a channel, levee and overbank complex in an ancient deep-water slope environment. *Sedimentary Geology* 132: 205-216.
- Di Giuseppe P, Agostini S, Lustrino M, Karaoğlu Ö, Savaşın MY et al. (2017). Transition from Compression to Strike-slip Tectonics Revealed by Miocene–Pleistocene Volcanism West of the Karlıova Triple Junction (East Anatolia). *Journal of Petrology* 58 (10): 2055-2087.
- Drooger CW (1983). Environmental gradients and evolutionary events in some larger foraminifera. In: Meulenkamp, JE (editor), *Utrecht Micropaleontological Bulletins* 30: 255-271.
- Dunham RJ (1962). Classification of carbonate rocks according to depositional texture. In: Ham WE (editor). *Classification of carbonate rocks. A symposium. American Association Petroleum Geologists Memoir* 1, pp. 108-121.
- Flügel E (2004). *Microfacies of Carbonate Rocks*. Berlin-Heidelberg, Germany: Springer.
- Hohenegger J (2000). Coenoclines of larger foraminifer. *Micropaleontology* 46 (1): 127-151.
- Hohenegger J (2004). Depth coenoclines and environmental considerations of western Pacific larger foraminifera. *Journal of Foraminiferal Research* 34 (1): 9-33.
- Hohenegger J (2005). Estimation of environmental paleogradient values based on presence/absence data: a case study using benthic foraminifera for paleodepth estimation. *Palaeogeography, Palaeoclimatology, Palaeoecology* 217: 115-130.
- Hottinger L (1977). *Foraminifères Operculiniformes*. Mémoires du Muséum National d'Histoire Naturelle, Paris, Nouvelle Série, 40, 1-159.
- Hottinger L (1997). Shallow benthic foraminiferal assemblages as signals for depth of their deposition and their limitations. *Bulletin de la Société Géologique de France* 168 (4): 491-505.
- Hottinger L (2000). Functional morphology of benthic foraminiferal shells, envelopes of cells beyond measure. *Micropaleontology* 46 (1): 57-86.
- Jorry SJ, Hasler CA, Davaud E (2006). Hydrodynamic behaviour of *Nummulites*, implications for depositional models. *Facies* 52: 221-235. doi: 10.1007/s10347-005-0035-z
- Kaya A (2016). Tectono-stratigraphic reconstruction of the Keban metamorphites based on new fossil findings, Eastern Turkey. *Journal of African Earth Sciences* 124: 245-257.
- Less Gy, Özcan E (2008). The late Eocene evolution of nummulitid foraminifer *Spiroclypeus* in the Western Tethys. *Acta Palaeontologica Polonica* 53 (2): 303-316.
- Less Gy, Özcan E, Papazzoni CA, Stockar R (2008). The middle to late Eocene evolution of nummulitid foraminifer *Heterostegina* in the Western Tethys. *Acta Palaeontologica Polonica* 53 (2): 317-350.
- Less Gy, Özcan E, Okay AI (2011). Stratigraphy and larger foraminifera of the middle Eocene to lower Oligocene shallow marine units in the northern and eastern parts of the Thrace Basin, NW Turkey. *Turkish Journal of Earth Sciences* 20: 793-845. doi: 10.3906/yer-1010-53
- Less Gy, Özcan E (2012). Bartonian-Priabonian larger benthic foraminiferal events in the Western Tethys. *Austrian Journal of Earth Sciences* 105 (1): 129-140.
- Less Gy, Frijia G, Özcan E, Saraswati PK, Parente M et al. (2018). Nummulitids, lepidocyclinids and Sr-isotope data from the Oligocene of Kutch (western India) with chronostratigraphic and paleobiogeographic evaluations. *Geodinamica Acta* 30 (1): 183-211. doi: 10.1080/09853111.2018.1465214
- Nebelsick JH, Rasser MW, Bassi D (2005). Facies dynamics in Eocene to Oligocene circumalpine carbonates. *Facies* 51: 197-216. doi: 10.1007/s10347-005-0069-2
- Özcan E, Less Gy, Baldi-Beke M, Kollányi K, Kertész B (2006). Biometric analysis of middle and upper Eocene Discocyclinidae and Orbitoclypeidae (Foraminifera) from Turkey and updated orthophragmine zonation in the Western Tethys. *Micropaleontology* 52 (6): 485-520.
- Özcan E, Less Gy (2009). First record of the co-occurrence of Western Tethyan and Indo-Pacific larger foraminifera in the Burdigalian of Eastern Turkey. *Journal of Foraminiferal Research* 39 (1): 23-39.
- Özcan E, Less Gy, Baldi-Beke M, Kollányi K, Acar F (2009a). Oligo-Miocene foraminiferal record (Miogypsinidae, Lepidocyclinidae and Nummulitidae) from the Western Taurides (SW, Turkey): biometry and implications for the regional geology. *Journal of Asian Earth Sciences* 34: 740-760.
- Özcan E, Less Gy, Baydoğan E (2009b). Regional implications of biometric analysis of Lower Miocene larger foraminifera from Central Turkey. *Micropaleontology* 55 (6): 559-588.
- Özcan E, Less Gy, Okay AI, Baldi-Beke M, Kollányi K et al. (2010). Stratigraphy and larger foraminifera of the Eocene shallow marine and olistostromal units of the southern part of the Thrace Basin, NW Turkey. *Turkish Journal of Earth Sciences* 19: 27-77. doi: 10.3906/yer-0902-11
- Özcan E, Okay AI, Bürkan KA, Yücel AO, Özcan Z (2018). Middle-Late Eocene marine record of the Biga Peninsula, NW Anatolia, Turkey. *Geologica Acta* 16 (2): 163-187.
- Özcan E, Less Gy, Jovane L, Catanzariti R, Frontalini F et al. (2019a). Integrated biostratigraphy of the middle to upper Eocene Kırkgeçit Formation (Baskil Section, Elazığ, Eastern Turkey): larger benthic foraminiferal perspective. *Mediterranean Geoscience Reviews* 1: 55-90.
- Özcan E, Yücel AO, Erbay S, Less Gy, Kaygılı S et al. (2019b). Reticulate *Nummulites* (*N. fabianii* Linage) and age of the *Pellatispira* beds of the Drazinda Formation, Sulaiman Range, Pakistan. *International Journal of Paleobiology & Paleontology* 2 (1): 1-10.
- Özkul M (1988). Elazığ batısında Kırkgeçit Formasyonu üzerinde sedimentolojik incelemeler. PhD, Fırat University, Elazığ, Turkey (in Turkish).
- Özkul M, Kerey İE (1996). Şelf, derin-deniz kompleksinde fasiyeler analizleri: Kırkgeçit Formasyonu (Orta Eosen- Oligosen), Baskil, Elazığ. *Tübitak, Journal of Earth Sciences* 5: 57-70 (in Turkish with English abstract).
- Papazzoni CA (1998). Biometric analyses of *Nummulites ptukhiani* Z. D. Kacharava, 1969 and *Nummulites fabianii* (Prever in Fabiani, 1905). *Journal of Foraminiferal Research* 28 (3): 161-176.
- Papazzoni CA, Cosovic V, Briguglio A, Drobné K (2017). Towards a calibrated larger foraminifera biostratigraphic zonation: celebrating 18 years of the application of shallow benthic zones. *Palaio* 32: 1-5. doi: 10.2110/palo.2016.043
- Perinçek D (1979). The Geology of Hazro-Korudağ, Çüngüş-Maden-Ergani-Hazar-Elazığ-Malatya region. Special Publications of the Geological Society of Turkey, Ankara, 33 pp.
- Pleş G, Kövecsi SA, Haitonic RB, Silye L (2020). Microfacies analysis and diagenetic features of the Eocene nummulitic accumulations from northwestern Transylvanian Basin (Romania). *Facies* 66: 20. doi: 10.1007/s10347-020-00604-x
- Racey A (1994). Biostratigraphy and palaeobiogeographic significance of Tertiary nummulitids (foraminifera) from Northern Oman. In: Simmons, MD (editor). *Micropalaeontology and Hydrocarbon Exploration in the Middle East*. London, Chapman-Hall, pp. 343-370.
- Racey A (1995). Lithostratigraphy and larger foraminiferal (nummulitid) biostratigraphy of the Tertiary of northern Oman. *Micropaleontology* 41: 1-123.

- Racey A (2001). A review of Eocene Nummulite accumulations: Structure, formation and reservoir potential. *Journal of Petroleum Geology* 24 (1): 79-100.
- Renema W (2018). Terrestrial influence as a key driver of spatial variability in large benthic foraminiferal assemblage composition in the Central Indo-Pacific. *Earth Science Reviews* 177: 514-544.
- Romero J, Caus E, Rosell J (2002). A model for the palaeoenvironmental distribution of larger foraminifera based on late Middle Eocene deposits on the margin of the South Pyrenean basin (NE Spain). *Palaeogeography, Palaeoclimatology, Palaeoecology* 179: 43-56.
- Saraswati PK, Anwar D, Lahiri A (2017). Bartonian reticulate *Nummulites* of Kutch. *Geodinamica Acta* 29 (2): 14-23. doi: 10.1080/09853111.2017.1300847
- Schaub H (1981). *Nummulites* et *Assilines* de la Téthys Paléogène. Taxinomie, phylogénese et biostratigraphie. *Memoires Suisses de Paleontologie* 104-106: 1-236 (in French).
- Serra-Kiel J, Hottinger L, Caus E, Drobne K, Ferrández-Cañadell C et al. (1998). Larger foraminiferal biostratigraphy of the Tetyan Paleocene and Eocene. *Bulletin de la Société Géologique de France* 169 (2): 281-299.
- Serra-Kiel J, Gallardo-Garcia A, Razin Ph, Robinet J, Roger J et al. (2016). Middle Eocene-Early Miocene larger foraminifera from Dhofar (Oman) and Socotra Island (Yemen). *Arabian Journal of Geosciences* 9: 344. doi: 10.1007/s12517-015-2243-3
- Seyrek A, Westaway R, Pringle M, Yurtmen S, Demir T et al. (2008). Timing of the Quaternary Elazığ volcanism, Eastern Turkey, and its significance for constraining landscape evolution and surface uplift. *Turkish Journal of Earth Sciences* 17: 497-541.
- Taşgın-Koç C, Nazik A, İslamoğlu Y, Türkmen İ (2012). Alt Pliyosen Çaybağı Formasyonu'nun faunal içeriği ve çökeltme ortamları ile ilişkisi, Elazığ Doğusu/Türkiye. *Hacettepe Üniversitesi Yerbilimleri Uygulama ve Araştırma Merkezi Bülteni* 33 (2): 99-130 (in Turkish with English abstract).
- Türkmen İ, İnceöz M, Aksoy E, Kaya M (2001). Elazığ yöresinin Eosen stratigrafisi ve paleocoğrafyası ile ilgili yeni bulgular. *Hacettepe Üniversitesi Yerbilimleri Bülteni* 24: 81-95 (in Turkish with English abstract).
- Yücel AO, Özcan E, Erbil Ü (2020). Latest Priabonian larger benthic foraminiferal assemblages at the demise of the Soğucak carbonate platform (Thrace basin and Black Sea shelf, NW Turkey): implications for the shallow marine biostratigraphy. *Turkish Journal of Earth Sciences* 29: 85-114. doi: 10.3906/yer-1904-19
- Zakrevskaya E, Less Gy, Bugrova E, Shcherbinina E, Grigoryan T et al. (2020). Integrated biostratigraphy and benthic foraminifera of the middle-upper Eocene deposits of Urtsadzor section (Southern Armenia). *Turkish Journal of Earth Sciences* 29: 896-945. doi: 10.3906/yer-1912-6